

Crystallization Behavior of Isotactic Propylene–Ethylene and Propylene–Butene Copolymers: Effect of Comonomers *versus* Stereodefects on Crystallization Properties of Isotactic Polypropylene

Claudio De Rosa,^{*,†} Finizia Auriemma,[‡] Odda Ruiz de Ballesteros,[‡] Luigi Resconi,[‡] and Isabella Camurati[‡]

Dipartimento di Chimica “Paolo Corradini”, Università di Napoli “Federico II”, Complesso Monte S. Angelo, Via Cintia, I-80126 Napoli, Italy, and Basell Polyolefins, Centro Ricerche G. Natta, P.le G. Donegani 12, I-44100 Ferrara, Italy

Received February 15, 2007; Revised Manuscript Received June 20, 2007

ABSTRACT: Isotactic propylene–ethylene (iPPeT) and propylene–butene (iPPBu) copolymers have been prepared with different metallocene catalysts. The different influences of stereodefects (isolated *rr* triads), ethylene and butene comonomeric units on the crystallization of the α and γ forms of isotactic polypropylene (iPP) have been discriminated. Both iPPeT and iPPBu copolymers crystallize from the melt as mixtures of the α and γ forms. The amount of the γ form increases with increasing crystallization temperature, comonomer concentration, and content of *rr* stereodefects. In iPPBu copolymers, the amount of the γ form decreases for concentration of butene units higher than 10–14 mol % and is always lower than that crystallized in iPPeT copolymers. Butene units, therefore, favor crystallization of the γ and α forms at low and high concentrations, respectively. These data have indicated that the crystallization of the γ form of iPP is not only related to the value of the average length of the regular propylene sequences $\langle L_{iPP} \rangle$, but is also related to the inclusion of stereodefects and constitutional defects in the crystals of iPP. Very different proportions of ethylene and butene units are included in crystals of the α and γ forms of iPP. Butene units are included indifferently in crystals of the α and γ forms, but probably more easily in the α form at high concentrations. Therefore, at low butene concentration, up to nearly 10 mol %, the effect of shortening of the length of regular isotactic propylene sequences prevails and induces crystallization of the γ form. For butene concentrations higher than 10 mol %, the effect of inclusion of butene units in crystals of the α form prevails, producing a decrease of the amount of the γ form and crystallization of the pure α form for butene contents higher than 30 mol %.

Introduction

Recent extensive investigations of the crystallization properties of isotactic polypropylene (iPP) produced with metallocene catalysts have demonstrated that the microstructure of the chains strongly influences the polymorphic behavior and the physical properties of iPP.^{1–19} Single-center metallocene catalysts allow a perfect control over the chain microstructure,²⁰ and iPP samples characterized by different kinds and amounts of *regio*- and *stereo*-irregularities can be produced.²⁰ Tailoring the chain microstructure affords opportunities for a fine-tuning of the physical properties, and iPP samples having different melting temperatures and properties of stiff plastic materials or elastomers can be obtained.^{12,16}

A unified view of the crystallization behavior of metallocene-made polypropylene has been recently suggested.^{9,11,12,16–19} iPP samples characterized by chains including different types of microstructural defects (stereodefects and regiodefects) generated by different catalysts generally crystallize as a mixture of the α and γ forms.^{1–19} The fraction of the γ forms increases with increasing crystallization temperature and the content of defects.^{1–3,6,8–10,12–18} Crystals of the γ form obtained in these samples always present structural disorder,^{7–9,11,12,16,19} characterized by a succession of bilayers of chains along a crystallographic direction with chain axes either parallel, as in the α form, or nearly perpendicular to each other, as in the γ form.^{7,9} The formation of the γ form seems to be favored by the presence of stereodefects (mainly *rr* isolated triads)^{1–3,6,8–12} and/or regiodefects (2,1 and 3,1 insertions)^{1–3,17} and also by the

presence of constitutional defects, such as comonomeric units.²¹ The most important parameter that influences the crystallization of the α and γ forms has been reported to be the average length of the regular isotactic propylene sequences.^{1–3,8,9,12,21} Short regular isotactic sequences would induce crystallization of the γ form.^{1–3,8–17} Since in metallocene-made iPPs the defects are randomly distributed along the polymer chains, even a small amount of defects shortens the length of the regular isotactic sequences, reducing the melting temperature and favoring the crystallization of the γ form.^{2,3,8,9,12,17} We found a linear relationship between the amount of the γ form that crystallizes from the melt and the average length of isotactic sequences.^{12,17} Moreover, the amount of the γ form strongly depends on the molecular mass because of the influence of the latter on the crystallization kinetics.^{17,18} It has been found that the crystallization of the γ form is favored for samples with high molecular mass because of the lower crystallization rate, at least in the range of molecular mass between 70 000 and 600 000.¹⁷

The influence of the presence of comonomeric units, on the crystallization of iPP has also been analyzed.^{21–67} Investigations on the structure and physical properties of polypropylene-based copolymers prepared with Ziegler–Natta catalysts are well-known and have been extensively reported in the less recent literature.^{21–38} It is well-known that with conventional Ziegler–Natta catalysts, comonomer incorporation is not uniform; thus, the lower-molecular weight fractions contain a higher percentage of comonomer and exhibit considerable solubility in hydrocarbons. The nonrandom distribution of comonomers and the presence of other types of microstructural defects prevented the study of the effects of the single comonomeric units on the crystallization behavior of iPP.

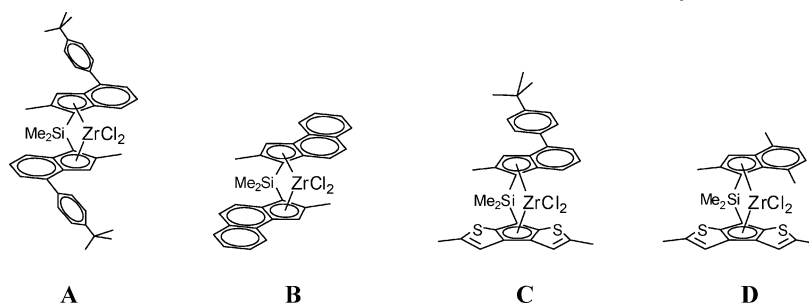
Copolymers prepared in recent years with metallocene catalysts are instead more chemically homogeneous, and show

* To whom correspondence should be addressed. Telephone: ++39 081 674346. Fax ++39 081 674090. E-mail: claudio.derosa@unina.it.

[†] Università di Napoli “Federico II”.

[‡] Basell Polyolefins.

Chart 1. Structures of Metallocenes Used in This Study



low levels of solubles even at relatively high comonomer incorporation.^{39–67} The advantage of using metallocene catalysts is that they afford incorporation of large contents of comonomer, copolymerization of cyclic and other comonomer types that are not easily incorporated with classical Ziegler–Natta catalysts, and excellent control of stereoregularity. In addition, metallocene catalysts may yield copolymers with a truly random comonomer distribution, uniform intermolecular distribution of the comonomer content, and narrow molecular weight distribution.

All the structural studies on both Ziegler–Natta^{21,25,27,30} and metallocene-based copolymers^{42,43,48–50} agree with the hypothesis that any comonomers induce a similar effect of shortening the regular isotactic sequences favoring the crystallization of the γ form over that of the α form. Alamo et al.⁴⁸ have found that the effect of the comonomer in enhancing the fractional content of the γ form is the same as the role of *stereo*- and *regio*-defects in the homopolymer chain. Thus, independent of the chemical nature of the comonomer, as the comonomer and/or crystallization temperature increase, the content of the γ form increases at the expense of the α phase.⁴⁸ However, differences in the partitioning of the ethylene, 1-butene, 1-hexene, and 1-octene units between the crystalline and noncrystalline regions leads to contents of the γ phase that differ among the copolymers because this produces different values of average length of the propylene sequences that crystallize.⁴⁸

To date, all the studies reported on metallocene-based iPP copolymers have allowed highlighting the different effects of different comonomers on the crystallization of the γ form of iPP,^{42–44,48–50,54,55} but could not discriminate between the influences of stereodefects and constitutional defects because in all published papers the copolymer samples have been prepared with only one type of metallocene catalyst and are, therefore, characterized by different contents of comonomeric units but a fixed concentration of *stereo*- and *regio*-defects.

In this paper we report a study of the crystallization properties and polymorphic behavior of isotactic propylene–ethylene (iPPet) and propylene–butene (iPPBu) copolymers prepared with metallocene catalysts of different *stereo*- and *regio*-selectivities. The chosen catalysts allow for the synthesis of copolymers with a well-defined microstructure, for instance samples with a very small concentration of stereodefects or regiodefects and variable amounts of comonomeric units or copolymers with similar concentration of comonomeric units but different concentration of *stereo*- and *regio*-defects.⁶⁵ This precise control of microstructure affords the opportunity to discriminate the effects of ethylene and butene comonomeric units and that of *rr* stereodefects on the crystallization behavior of iPP.

Experimental Section

All iPP homopolymer samples and iPPet and iPPBu copolymer samples have been prepared at temperatures between 60 and 70 °C in liquid monomers, with the four metallocenes shown in Chart 1, activated with methylalumoxane (MAO). The two C_2 -symmetric

metallocenes **A** and **B** are not completely regioselective, with **A** being almost fully isoselective^{68,69} and **B**⁷⁰ less isoselective than **A**. On the other hand, the two C_1 -symmetric metallocenes **C** and **D** are fully regioselective but not perfectly isoselective, with **D** being less isoselective than **C**.⁷¹ The MAO-activated metallocenes were supported on spherical SiO_2 particles, or on porous polyethylene or polypropylene particles following a Basell proprietary technology.⁷²

The microstructural data of all samples have been obtained from ^{13}C NMR analysis. All spectra were obtained using a Bruker DPX-400 spectrometer operating in the Fourier transform mode at 120 °C at 100.61 MHz. The samples were dissolved with a 8 wt %/v concentration in 1,1,2,2-tetrachloroethane- d_2 at 120 °C. The carbon spectra were acquired with a 90° pulse and 12 s of delay between pulses and CPD (WALTZ 16) to remove ^1H – ^{13}C coupling. About 1500–3000 transients were stored in 32K data points using a spectral window of 6000 Hz. For iPP samples, the peak of the *mmmm* pentad in the ^{13}C spectra (21.8 ppm) was used as a reference. For propylene–ethylene copolymers, the assignments of the peaks were made according to Randall⁷³ and Tritto et al.⁷⁴ and the triad distribution and copolymer compositions were determined according to Kakugo.⁷⁵ The $P_{\beta\beta}(\text{mm})$ peak at 21.8 ppm (nomenclature according to Randall⁷³) was used as internal reference. The product of reactivity ratios $r_P \times r_E$ was calculated from the triads according to Carman et al.,⁷⁶ adapted for propylene-rich copolymers (P = propylene; E = ethylene).

$$r_P \times r_E = 1 + \left(\frac{\text{EEE} + \text{PEE}}{\text{PEP}} + 1 \right) - \left(\frac{P}{E} + 1 \right) \left(\frac{\text{EEE} + \text{PEE}}{\text{PEP}} + 1 \right)^{0.5}$$

The tacticity of propylene sequences was calculated as PPP_{mm} content from the ratio of the $T_{\beta\beta}(\text{mm})$ (28.74–28.45 ppm) and the whole $T_{\beta\beta}$ (28.74–28.30 ppm).

For the ^{13}C NMR of iPPBu copolymers, each spectrum was acquired with 15 s of delay between pulses. The assignments of the resonances and the 1-butene content for the propylene–butene copolymers were determined from the diad distribution, from the $S_{\alpha\alpha}$ carbons, according to Randall.⁷⁷ The peak of the propylene methine carbon atoms was used as internal reference at 28.83 ppm. The evaluation of diad distribution and the composition was obtained from the $S_{\alpha\alpha}$ peaks using the following equations (P = propylene; B = butene):

$$\text{BB} = 100S_{\alpha\alpha}(\text{BB})/\Sigma S_{\alpha\alpha}$$

$$\text{PB} = 100S_{\alpha\alpha}(\text{PB})/\Sigma S_{\alpha\alpha}$$

$$\text{PP} = 100S_{\alpha\alpha}(\text{PP})/\Sigma S_{\alpha\alpha}$$

$$[P] = \text{PP} + 0.5\text{PB}$$

$$[B] = \text{BB} + 0.5\text{PB}$$

The product of reactivity ratios $r_P \times r_B$ was determined from the diads according to Kakugo et al.,⁷⁵ $r_P \times r_B = 4[\text{PP}] \times [\text{BB}]/[\text{PB}]^2$.

The iPP homopolymer samples are described in Table 1, whereas the iPPet and iPPBu copolymers are described in Tables 2 and 3, respectively. We have used the designation YEX or YBX, where Y is the symbol of the metallocene (**A**, **B**, **C**, **D**) and X is the molar

Table 1. Weight-Average Molecular Masses (\bar{M}_w), Polydispersities (\bar{M}_w/\bar{M}_n), Melting Temperatures of As-Prepared Samples (T_m), Contents of Stereoerrors (rr), Concentrations of Secondary 2,1-Erythro Units (2,1e), and Total Concentration of Defects (ϵ) of the iPP Homopolymer Samples Prepared with the MAO Activated Metallocenes A–D (Chart 1)

sample	catalyst/cocatalyst/carrier ^a	\bar{M}_w	\bar{M}_w/\bar{M}_n	T_m (°C) ^b	$[rr]$ (%) ^c	[2,1e] (%) ^d	ϵ (%) ^e
iPPA	A/MAO/PE	237 500	2.2	151	0.2	0.8	1.0
iPPB	B/MAO/PE	254 600	2.0	147	1.0	0.7	1.7
iPPC	C/MAO/PE	142 400	2.2	140	2.5	<0.1	2.5
iPPD	D/MAO/PP	247 000	2.3	133	3.5	<0.1	3.5

^a PE = polyethylene, PP = polypropylene. ^b Melting temperatures of as-prepared samples from DSC scans at heating rate of 10 °C/min. ^c $[rr]$ is the percentage of primary stereoerrors over all monomer units, $[rr] = [mrrm] + [mrrr]$. ^d Secondary insertions 2,1 are only of the erythro type, and their amount is also normalized over all monomer units. ^e $\epsilon = [rr] + [2,1e]$.

Table 2. Weight-Average Molecular Masses (\bar{M}_w), Polydispersities (\bar{M}_w/\bar{M}_n), Melting Temperatures of As-Prepared Samples (T_m), Concentration of Ethylene Comonomeric Units (mol %), Products of Reactivity Ratios ($r_P \times r_E$), Contents of Stereoerrors (rr), Concentrations of Secondary 2,1-Erythro Units (2,1e), and Total Concentration of Defects (ϵ) of the Isotactic Propylene–Ethylene Copolymers Prepared with the MAO Activated Metallocenes A and D of Chart 1, Where the Homopolymer Data from Table 1 Are Also Included for Comparison

sample	catalyst/cocatalyst/carrier ^a	\bar{M}_w	\bar{M}_w/\bar{M}_n	T_m (°C) ^b	mol % ethylene	$r_P \times r_E$ ^c	$[rr]$ (%) ^d	[2,1e] (%) ^e	ϵ (%) ^f
iPPA	A/MAO/PE	237 500	2.2	151	0	n.d.	0.2	0.8	1.0
AE0.6	A/MAO/PE	n.d.	n.d.	145	0.6	n.d.	n.d.	0.7	1.5
AE4	A/MAO/PE	292 800	2.1	127	4.0	1.3	n.d.	0.6	4.8
AE7.4	A/MAO/PE	288 600	2.1	112	7.4	2.0	n.d.	0.4	8.0
iPPD	D/MAO/PP	247 000	2.3	133	0	n.d.	3.5	<0.1	3.5
DE3.6	D/MAO	n.d.	n.d.	116	3.6	1.6	3.6	0	7.2
DE13.1	D/MAO	193 400	2.0	55	13.1	1.2	3.2	0	16.3

^a PE = polyethylene. ^b Melting temperatures of as-prepared samples from DSC scans at heating rate of 10 °C/min. ^c Calculated according to ref 76. ^d $[rr]$ is the percentage of primary stereoerrors over all monomer units, $[rr] = [mrrm] + [mrrr]$. The content of stereoerrors in the copolymers from A/MAO/PE is not determinable and is assumed to be the same as that found in the corresponding homopolymer iPPA. ^e Secondary insertions 2,1 are only of the erythro type, and their amount is also normalized over all monomer units. [2,1e] is the sum of the concentrations of isolated secondary 2,1-Erythro units (PSP, P = propylene, S = secondary 2,1 propylene unit) and secondary 2,1e units after ethylene insertion (PESP, E = Ethylene). [PSP] and [PESP] are 0.6% and 0.08%, respectively, for the sample AE0.6, 0.27% and 0.31%, respectively, for the sample AE4.0, and 0.09% and 0.29%, respectively, for the sample AE7.4. ^f $\epsilon = [rr] + [2,1e] + [\text{ethylene}]$. n.d. = not determinable.

Table 3. Weight-Average Molecular Masses (\bar{M}_w), Polydispersities (\bar{M}_w/\bar{M}_n), Melting Temperatures of As-Prepared Samples (T_m), Concentration of Butene Comonomeric Units (mol %), Products of Reactivity Ratios ($r_P \times r_B$), Contents of Stereoerrors (rr), Concentrations of Secondary 2,1-Erythro Units (2,1e), and Total Concentration of Defects (ϵ) of the Isotactic Propylene–Butene Copolymers Prepared with the MAO Activated Metallocenes A–D (Chart 1), Where the Homopolymer Data from Table 1 Are Also Included for Comparison

sample	catalyst/cocatalyst/carrier ^a	\bar{M}_w	\bar{M}_w/\bar{M}_n	T_m (°C) ^b	mol % butene	$r_P \times r_B$ ^c	$[rr]$ (%) ^d	[2,1e] (%) ^e	ϵ (%) ^f
iPPA	A/MAO/PE	237 500	2.2	151	0	n.d.	0.2	0.8	1.0
AB1.9	A/MAO/SiO ₂	316 500	2.2	143	1.9	n.d.	<0.1	0.5	2.4
AB4.3	A/MAO/PE	228 700	2.1	137	4.3	1.0	<0.1	0.4	4.7
AB4.4	A/MAO/SiO ₂	207 000	2.0	138	4.4	0.8	<0.1	0.5	4.9
AB8.2	A/MAO/PE	178 500	2.0	125	8.2	0.9	<0.1	0.2	8.4
AB8.3	A/MAO/SiO ₂	200 000	2.1	120	8.3	0.9	<0.1	0.3	8.6
AB13.6	A/MAO/SiO ₂	161 500	2.4	110	13.6	0.8	<0.1	0.1	13.7
iPPB	B/MAO/PE	254 600	2.0	147	0	-	1.0	0.7	1.7
BB1.6	B/MAO/PE	225 000	2.0	138	1.6	n.d.	1.0	0.6	3.2
BB2.8	B/MAO/PE	251 600	2.0	132	2.8	n.d.	1.0	0.5	4.3
BB3.7	B/MAO/PE	225 700	2.0	130	3.7	1.6	0.8	0.6	5.0
BB6.0	B/MAO/PE	229 000	2.0	123	6.0	1.4	0.7	0.3	7.1
iPPC	C/MAO/PE	142 400	2.2	140	0	n.d.	2.5	<0.1	2.5
CB1.3	C/MAO/PE	172 900	2.1	135	1.3	n.d.	2.4	n.v.	3.7
CB4.6	C/MAO/PE	175 700	2.0	123	4.6	n.d.	2.4	n.v.	7.0
CB8.2	C/MAO/PE	176 700	2.0	112	8.2	1.2	1.9	n.v.	10.1
iPPD	D/MAO/PP	247 000	2.3	133	0	n.d.	3.5	<0.1	3.5
DB1.4	D/MAO/PE	214 000	2.1	126	1.4	n.d.	3.4	<0.1	4.8
DB2.2	D/MAO/PE	214 500	2.0	124	2.2	n.d.	3.4	n.v.	5.6
DB6.4	D/MAO/PE	214 400	2.0	113	6.4	1.0	2.5	n.v.	8.9
DB17.9	D/MAO	368 400	3.1	85	17.9	0.9	2.2	n.v.	20.1
DB36.4	D/MAO	204 000	2.7	67	36.4	n.d.	2.2	n.v.	38.6

^a PE = polyethylene; PP = polypropylene. ^b Melting temperatures of as-prepared samples from DSC scans at heating rate of 10 °C/min. ^c Calculated from $r_P \times r_B = (4[PP] \times [BB])/[PB]^2$ according to ref 75. ^d $[rr]$ is the percentage of primary stereoerrors over all monomer units, $[rr] = [mrrm] + [mrrr]$. ^e Secondary insertions 2,1 are only of the erythro type, and their amount is also normalized over all monomer units. ^f $\epsilon = [rr] + [2,1e] + [\text{butene}]$. n.d. = not determinable. n.v. = not visible.

content of ethylene (E) or butene (B) units in the copolymers. Narrow molecular weight distributions and $r_1 \times r_2$ values close to 1 are good indicators of narrow comonomer distributions in the copolymers. The mass average molecular masses were evaluated from size exclusion chromatography (SEC).

The calorimetric measurements were performed with a differential scanning calorimeter (DSC) Perkin-Elmer DSC-7 in a flowing N₂ atmosphere (see Supporting Information). Densities were measured by flotation of compression-molded films at 25 °C in solutions of water and ethyl alcohol.

The various iPP homopolymer and copolymer samples were isothermally crystallized from the melt at different temperatures. Powder samples were melted at 200 °C and kept for 5 min at this temperature in a N₂ atmosphere; they were then rapidly cooled to the crystallization temperature, T_c , and kept at this temperature, still in a N₂ atmosphere, for a time long enough to allow complete crystallization at T_c . The samples were then rapidly cooled to room temperature and analyzed by X-ray diffraction. In the various isothermal crystallizations, the crystallization time t_c is different depending on the crystallization temperature. The shortest time is

24 h for the lowest crystallization temperatures and increases with increasing the crystallization temperature, up to 2 weeks for the highest crystallization temperatures.

X-ray powder diffraction profiles were obtained with Ni-filtered Cu K α radiation with an automatic Philips diffractometer. The relative amount of crystals in the γ form present in our samples was determined from the X-ray diffraction profiles, by measuring the ratio between the intensities of the (117) $_{\gamma}$ reflection at $2\theta = 20.1^\circ$, typical of the γ form,⁷⁸ and the (130) $_{\alpha}$ reflection at $2\theta = 18.6^\circ$, typical of the α form:⁷⁹ $f_{\gamma} = I(117)_{\gamma}/[I(130)_{\alpha} + I(117)_{\gamma}]$. The intensities of (117) $_{\gamma}$ and (130) $_{\alpha}$ reflections were measured from the area of the corresponding diffraction peaks above the diffuse amorphous halo in the X-ray powder diffraction profiles. The amorphous halo has been obtained from the X-ray diffraction profile of an atactic polypropylene, and then it was scaled and subtracted to the X-ray diffraction profiles of the melt-crystallized samples. The indices of crystallinity (x_c) were evaluated from the X-ray powder diffraction profiles by the ratio between the crystalline diffraction area (A_c) and the total area of the diffraction profile (A_t), $x_c = A_c/A_t$. The crystalline diffraction area has been obtained from the total area of the diffraction profile by subtracting the amorphous halo.

Conformational and packing energy calculations have been performed with the software package⁸⁰ CERIU²,² using the force field indicated as PCFF⁸¹ in the CERIU² program. A cutoff distance of 4 Å for attractive nonbonded interactions and for Coulombic interactions (dielectric constant, $\epsilon = 1$) was selected, and a spline function has been used from 4 to 5 Å to attenuate gradually the interaction energy from its full value to zero. No interactions over 5 Å have been taken into account.

Defects have been introduced in the central portion of molecular models of a iPP chain in 3/1 helical conformation constituted by 9 and/or 12 monomeric units and the packing energy has been minimized with respect to the positions of the atoms in the defective portion of the chain by placing the model oligomer in a cluster of close neighboring chains free of defects, packed as in the α and/or γ forms of iPP according to the space groups $P2_1/c$ ⁸² and $Fd2d$,⁷⁸ respectively. The atomic position of atoms aside the defect has been fixed during the minimization. Since the environment of the chains is not 3₁ symmetric, minimizations have been carried out by placing the defect in the three consecutive positions over one turn of the helix and only the conformations corresponding to the lowest conformational and packing energy are reported. The values of conformational energy that nearly correspond to the total energy, because for the considered models of chains the values of the packing energy are very low, are given with respect to the energy of a defect-free model chain of iPP in 3₁ helical conformation.

Results and Discussion

As-Prepared Samples. Samples of iPP homopolymer and iPPet and iPPBu copolymers prepared with catalysts **A** and **B** are highly stereoregular and contain only very small amounts of stereoerrors and regiodeflects, due to secondary 2,1 erythro units (2,1e). The stereoerrors are identified by the *rr* triad defects. Catalyst **A** is more isoselective than **B** and produces iPP homopolymers with about 0.2 mol % of isolated *rr* defects and 0.8 mol % of 2,1e regiodeflects (Table 1). Homopolymer samples prepared with catalyst **B** contain slightly higher amount of *rr* defects (about 1 mol %) and lower concentration of regiodeflects ([2,1e] = 0.7%). Homopolymer samples prepared with catalysts **C** and **D** of Chart 1 are highly regioregular (no 2,1 regiodeflects are detectable) but less stereoregular and, therefore, contain only errors in the stereoregularity.⁷¹ The concentrations of stereoerrors *rr* in these samples (iPPC and iPPD) are 2.5 and 3.5 mol %, respectively (Table 1), and they correspond to the percentage of primary stereoerrors over all monomer units, $[rr] = [mrrm] + [mrrr]$. These concentrations are much higher than those in the samples prepared with catalysts **A** and **B**.

All catalysts produce iPPet and iPPBu copolymer samples with microstructures similar to those of the homopolymer samples prepared with the same catalyst. Examples of ¹³C NMR spectra are reported in the Supporting Information. However, both concentrations of *rr* stereoerrors and 2,1e regiodeflects are not constant with the comonomer concentration (Tables 2 and 3). In particular, for iPPBu copolymers the concentrations of *rr* defects and 2,1e regiodeflects decrease with increasing butene content (Table 3). As a result, samples of iPPBu copolymers with high butene content prepared with catalysts **A** and **B** have very high stereoregularity. Catalyst **A** is, indeed, almost fully isoselective for iPPBu copolymers (Table 3). For iPPet copolymers prepared with catalyst **A**, the content of stereoerrors is not determinable and is assumed to be the same as that found in the corresponding homopolymer iPPA (Table 2).

These particular microstructures of iPPet and iPPBu copolymers allow for the comparison of samples containing very small concentration of stereoerrors or regiodeflects and variable amounts of comonomeric units or copolymers with similar concentration of comonomeric units but different concentration of *stereo*- and *regio*-defects. This, in turn, affords a unique opportunity for studying the influence of constitutional defects on the crystallization behavior of iPP and discriminating the effects of different comonomers and stereoerrors on the polymorphic behavior of iPP.

The X-ray powder diffraction profiles of as-prepared samples of iPPet and iPPBu copolymers, compared with those of the corresponding iPP homopolymer samples prepared with the same catalysts, are reported in Figure 1. All homopolymer samples crystallize in the α form, as indicated by the presence of the (130) $_{\alpha}$ reflection at $2\theta = 18.6^\circ$ of the α form,⁷⁹ and the absence of the (117) $_{\gamma}$ reflection at $2\theta = 20.1^\circ$ of the γ form,⁷⁸ in the X-ray powder diffraction profile *a* of Figure 1A–F. However, the low intensity of the (130) $_{\alpha}$ reflection indicates that α/γ disordered modifications intermediate between α and γ forms have been obtained.^{8,9,11} All iPPet and iPPBu copolymer samples are crystallized as mixtures of the α and γ forms of iPP, as indicated by the presence of both (130) $_{\alpha}$ and (117) $_{\gamma}$ reflections at $2\theta = 18.6$ and 20.1° of the α and γ forms, respectively, in the diffraction profiles of Figure 1.

In both iPPet and iPPBu copolymers, the amount of crystals of the γ form, with respect to that of the α form, increases with increasing concentration of comonomers, as indicated by the increase of the intensity of the (117) $_{\gamma}$ reflection of the γ form in the diffraction profiles of Figure 1A–F. In the case of iPPBu copolymers this is true only up to butene concentration of 10–15 mol % (Figure 1C–F). The data of Figure 1F show, indeed, that the intensity of the (117) $_{\gamma}$ reflection of the γ form decreases for butene contents higher than nearly 15 mol %, indicating a decrease of the amount of the γ form, and is zero in the diffraction profile of sample having 36.4 mol % of butene units, which is crystallized in the pure α form (profile *f* of Figure 1F).

It is well-known that iPPBu copolymers crystallize in the whole range of composition, up to 100% of butene content.^{22,35,41} Samples having concentration of butene units up to about 50 mol % crystallize in the polymorphic forms of iPP, whereas samples of iPPBu copolymers with butene content higher than 65–70 mol % show crystallinity arising from crystallization of isotactic polybutene (iPB). iPP and iPB cocrystallize in iPPBu samples with similar concentrations of propylene and butene units (in the range 50–60 mol % of butene). The data of Figure 1 indicate that samples of iPPBu copolymers showing iPP crystallinity, with butene content lower than 50 mol %, are

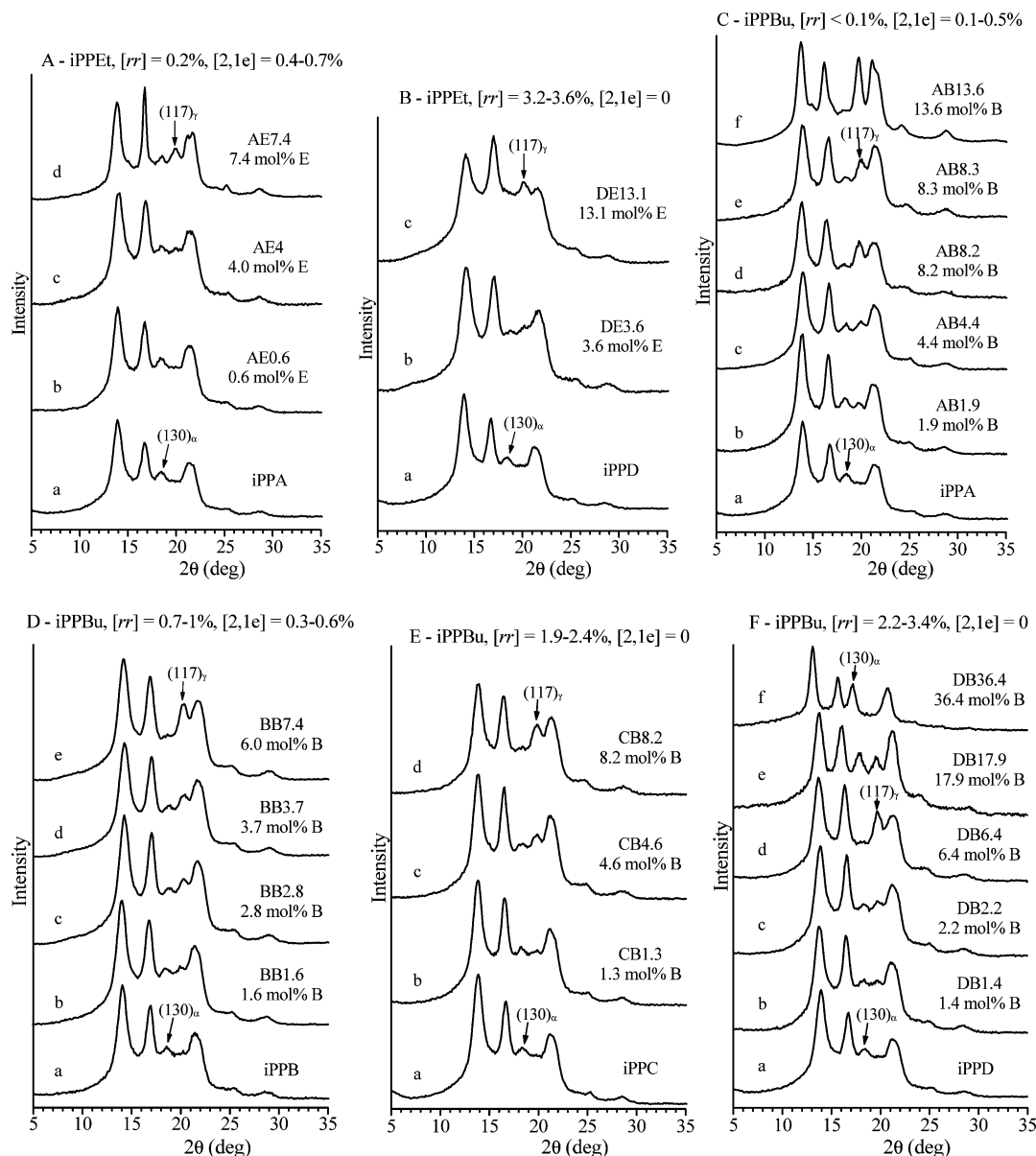


Figure 1. X-ray powder diffraction profiles of as-prepared samples of iPPet copolymers prepared with catalysts **A** (A) and **B** (B) and iPPBu copolymers prepared with catalysts **C** (C), **B** (D), **C** (E), and **D** (F). The diffraction profiles of iPP homopolymer samples prepared with the same catalysts (profiles a in A–F) are also reported. The $(130)_\alpha$ and $(117)_\gamma$ reflections at $2\theta \approx 18.6$ and 20° , respectively, of the α and γ forms of iPP, respectively, are indicated. The concentrations (mol %) of ethylene (E) and butene (B) units are also indicated.

crystallize in the α and γ forms of iPP, or as a mixture of both, the γ form being favored for low butene concentrations, up to nearly 15 mol % (Figure 1C–F). The α form is instead favored at higher butene concentration and samples with butene content higher than 20–30 mol % are crystallized in the pure α form (profile f of Figure 1F).

The fraction of the γ form for as-prepared samples of iPPet and iPPBu copolymers is reported in Figure 2 as a function of comonomer concentration (Figure 2, parts A and C, respectively) and of the total concentration of defects ϵ , defined as the sum of concentrations of rr stereodefects, 2,1 regiodefects, and comonomeric units (Figure 2, parts B and D). It is apparent that for all samples the amount of the γ form increases with increasing comonomer concentration, and decreases in the case of iPPBu samples with butene contents higher than 15–16 mol % (Figure 2C). Moreover, for similar concentrations of butene or ethylene units, the amount of the γ form is higher in more stereoregular copolymer samples prepared with catalysts **C** and **D**, containing high amount of rr defects (1.9–3.6%), than

in highly isotactic samples prepared with catalysts **A** and **B** (Figure 2A,C), containing negligible amounts of rr defects (Tables 2 and 3). These data indicate that, as already demonstrated in the literature,^{1–3,8–12} either rr stereodefects^{3,12} and 2,1 regiodefects,^{1–3,17} or constitutional defects (comonomeric units)^{22a,25,27,30,42,43,48–50} induce crystallization of the γ form. Therefore, for samples containing a non-negligible concentration of rr stereodefects, the effect of the presence of constitutional defects is added to the contribution due to the presence of stereodefects.

However, for both iPPet and iPPBu copolymers the data of fraction of the γ form as a function of the total concentration of defects ($\epsilon = [rr] + [2,1e] + [\text{comonomeric units}]$) are fitted by single curves (Figure 2B,D) indicating that rr stereodefects and comonomeric units exert a similar effects on the crystallization of the γ form, at least in conditions of fast kinetic-controlled crystallization from the polymerization medium of as-prepared samples. Therefore, from these data, it is still

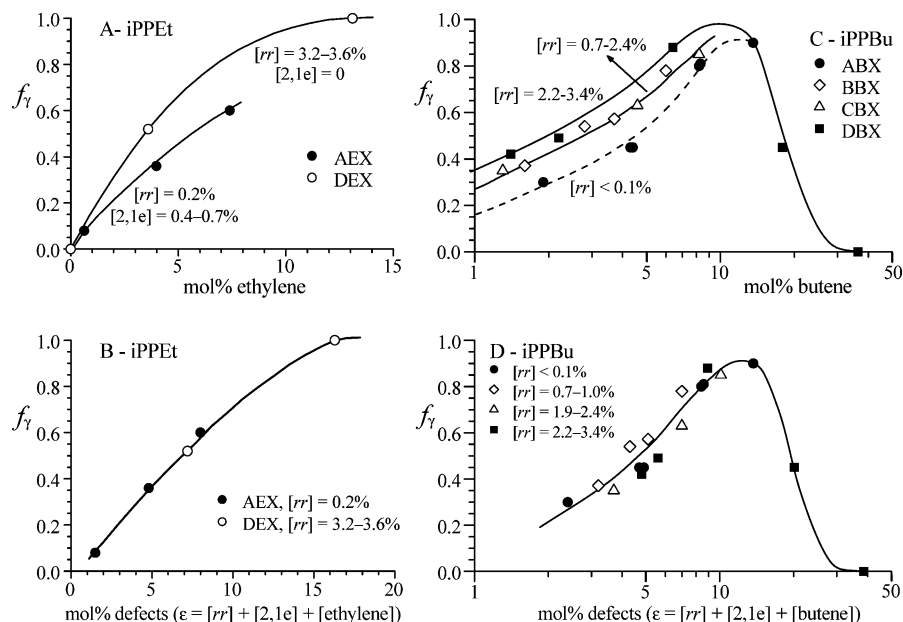


Figure 2. Relative amounts of the γ form (f_γ) in as-prepared samples of iPPet (A,B) and iPPBu (C,D) copolymers as a function of ethylene (A) or butene concentrations (C), and of the total concentration of defects ϵ (B,D), that is, the sum of concentrations of rr stereodefects, 2,1e regiodefects, and comonomeric units. (A,B) samples iPPet prepared with the catalysts A with $[rr] = 0.2\%$ (●) and D with $[rr] = 3.2-3.6\%$ (○). (C,D) samples iPPBu prepared with catalysts A with $[rr] < 0.1\%$ (●), B with $[rr] = 0.7-1\%$ (◇), C with $[rr] = 1.9-2.4\%$ (△) and D with $[rr] = 2.2-3.4\%$ (■).

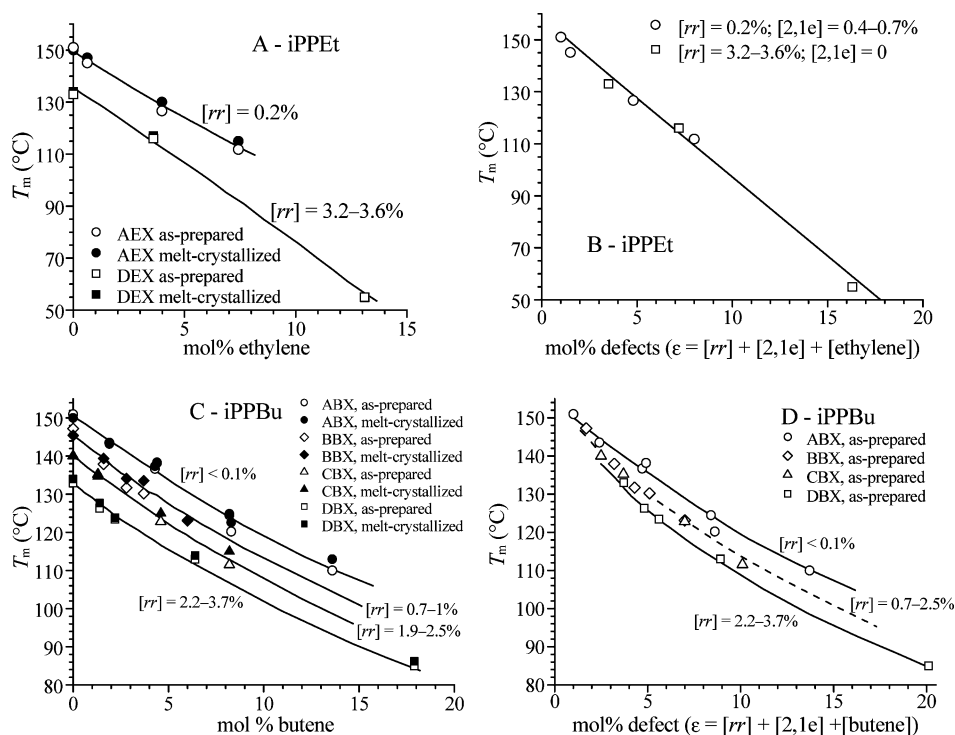


Figure 3. Melting temperatures (T_m) of samples of iPPet (A,B) and iPPBu (C,D) copolymers as a function of ethylene (A) or butene (C) concentrations, and of the total concentration of defects ϵ (B,D), that is, the sum of concentrations of rr stereodefects, 2,1e regiodefects and comonomeric units. (A,B) as-prepared (○,□) and melt-crystallized (●,■) samples of iPPet copolymers prepared with the catalysts A with $[rr] = 0.2\%$ (○, ●) and D with $[rr] = 3.2-3.6\%$ (□, ■). (C,D) as-prepared (open symbols) and melt-crystallized (filled symbols) samples of iPPBu copolymers prepared with catalysts A with $[rr] < 0.1\%$ (○, ●), B with $[rr] = 0.7-1.0\%$ (◇, ◆), C with $[rr] = 1.9-2.4\%$ (△, ▲) and D with $[rr] = 2.2-3.4\%$ (□, ■). The values of melting temperatures of iPP homopolymer samples prepared with the same catalysts are also reported at zero comonomer concentration.

difficult to discriminate the role played by stereodefects and constitutional defects and discriminate between the effects of ethylene and butene units. Only at very high concentrations of comonomeric units (higher than 15 mol %) are the effects of ethylene and butene clearly different. Butene units favor crystallization of the α form (Figure 2C,D) and do not prevent crystallization (Figure 1F), whereas ethylene induces crystallization of the pure γ form (Figure 2B), although with high

degree of structural disorder (curve c of Figure 1B), and prevents crystallization for ethylene concentrations higher than 20–25 mol %.⁵⁴

The melting temperatures of as-prepared and melt-crystallized (by cooling the melt to room temperature at cooling rate of 10 °C/min) samples of iPPet and iPPBu copolymers are reported in Figure 3 as a function of comonomer concentration (Figure 3A,C) and of the total concentration of defects $\epsilon = [rr] + [2,1e] + [\text{comonomer}]$ (Figure 3B,D).

1e] + [comonomer] (Figure 3B,D). It is apparent that the melting temperature decreases with increasing ethylene or butene concentration (Figure 3A,C). In both iPPeT and iPPBu copolymers, for similar amounts of comonomeric units (ethylene or butene), the melting temperature decreases with decreasing stereoregularity (Figure 3A,C). Lower melting temperatures are observed for samples of iPPeT and iPPBu copolymers with higher concentrations of *rr* defects (Figure 3, parts A and C).

However, in the case of iPPeT copolymers the data of melting temperatures as a function of the total concentration of defects ($\epsilon = [rr] + [2,1e] + [\text{ethylene}]$) are fitted by a single straight line (Figure 3B), indicating that *rr* stereodefects and ethylene comonomeric units exert similar effects in decreasing the melting temperature of polypropylene.

Samples of iPPBu copolymers having the same total concentration of defect ($\epsilon = [rr] + [2,1e] + [\text{butene}]$) present, instead, different melting temperatures (Figure 3D). In particular, more stereoirregular samples containing high content of *rr* defects (samples DBX with $[rr] = 2.2\text{--}3.4\%$), show melting temperatures lower than those of more stereoregular samples with similar values of ϵ , containing lower *rr* content but higher concentration of butene (for instance samples ABX with $[rr] < 0.1\%$). This indicates that *rr* stereodefects and butene comonomeric units exert different effects in decreasing the melting temperature of polypropylene, the disturbance of butene units being lower than that due to the presence of *rr* triad stereodefects.

Moreover, the comparison of melting temperatures of iPPeT and iPPBu samples AEX and ABX or DEX and DBX prepared with the same catalysts (A and D), therefore, containing similar concentrations of *rr* and 2,1 defects, clearly indicates that iPPBu copolymers always present melting temperatures higher than those of iPPeT copolymers of similar concentration of comonomer.

The degree of crystallinity of iPPeT and iPPBu copolymers, evaluated from the X-ray diffraction profiles of Figure 1, are reported in Figure 4 as a function of the comonomer concentration. For iPPeT copolymers the crystallinity decreases with increasing ethylene concentration, whereas all iPPBu copolymer samples present a high degree of crystallinity, around 50%, that does not greatly change with the butene concentration, at least up to nearly 14–15 mol % (Figure 4A). A slight decrease of crystallinity is observed only for butene contents higher than 15–16 mol % (Figure 4A).

The data of melting temperature (Figure 3) and crystallinity (Figure 4) indicates that butene units produce less disturbance of the crystallization of iPP than that produced by ethylene units, notwithstanding the bigger size, and even less than that of *rr* stereodefects. This is also confirmed in Figure 4B where the melting temperatures of iPP homopolymer samples of different stereoregularity, containing only *rr* defects,¹² are compared with those of iPPeT and iPPBu copolymers. It is apparent that whereas iPPeT copolymers present melting temperatures similar to those of stereodeficient iPP homopolymers, iPPBu copolymers show melting temperatures higher than those of both homopolymers and iPPeT copolymers.

This different behavior may be related to the inclusion of comonomers in crystals of the α and γ forms of iPP and their different compatibility with the crystalline lattices that may produce different proportions of ethylene and butene units included in crystals of the α and γ forms.^{5,21–23,25,27b,33,35,41,47,56}

For our iPPeT copolymer samples, we have not observed changes of the values of the Bragg distances of equatorial reflections in the X-ray powder diffraction profiles of Figure

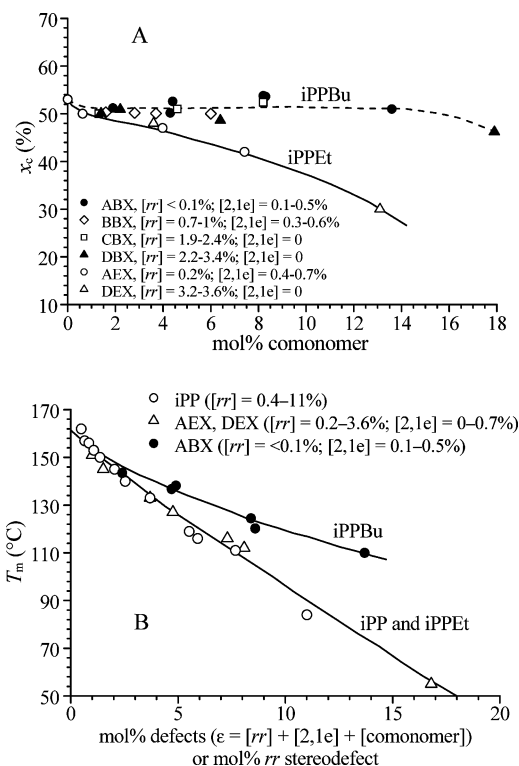


Figure 4. (A) Degree of crystallinity (x_c) of as-prepared samples of iPPBu copolymers prepared with catalysts A with $[rr] < 0.1\%$ (●), B with $[rr] = 0.7\text{--}1.0\%$ (◇), C with $[rr] = 1.9\text{--}2.4\%$ (□) and D with $[rr] = 2.2\text{--}3.4\%$ (▲) and of iPPeT copolymers prepared with the catalysts A with $[rr] = 0.2\%$ (○) and D with $[rr] = 3.2\text{--}3.6\%$ (△) as a function of comonomer concentration. (B) Melting temperature (T_m) of as-prepared samples of iPPBu copolymers prepared with the catalyst A with $[rr] < 0.1\%$ (●) and of iPPeT copolymers prepared with the catalysts A with $[rr] = 0.2\%$ and D with $[rr] = 3.2\text{--}3.6\%$ (△), compared with the melting temperatures of samples of iPP homopolymer (○) of different stereoregularity containing variable amount of *rr* stereodefects, reported as a function of total concentration of defects ϵ (in the case of iPP homopolymers $\epsilon = [rr]$).

1A,B with the ethylene concentration. In the case of as-prepared and melt-crystallized samples of iPPBu copolymers, which crystallize as mixtures of the α and γ forms, the increase of butene concentration induces, instead, an increase of the Bragg distances of equatorial reflections of both crystals of α and γ forms (Figure 1C–F).

The values of Bragg distances of $(110)_\alpha$, $(040)_\alpha$, and $(111)_\alpha$ reflections of the α form and $(111)_\gamma$, $(008)_\gamma$, and $(202)_\gamma$ reflections of the γ form, which occur at $2\theta \approx 14$, 17, and 21° , respectively, in the diffraction patterns of the α and γ forms of iPP homopolymer, are reported in Figure 5A. It is apparent that at low butene contents, up to 10–14 mol %, the Bragg distances of $(110)_\alpha$ and $(111)_\alpha$ reflections of the α form and of $(111)_\gamma$ and $(202)_\gamma$ reflections of the γ form are nearly constant, whereas the Bragg distance of the $(040)_\alpha$ reflection of the α form, or $(008)_\gamma$ reflection of the γ form, slightly increases with increasing butene concentration (Figure 5A).

This indicates an appreciable increase of the dimension of the b_α axis of the monoclinic unit cell of the α form and of the c_γ axis of the orthorhombic unit cell of the γ form with increasing butene concentration (Figure 5B) and inclusion of butene comonomeric units in both crystals of the α and γ forms of iPP.^{21,22c,35,27b,56} Inclusion of butene units in crystals of the α and γ forms mainly produces increase of b_α and c_γ axes of crystals of the α and γ forms, respectively, which correspond, in both the α and γ forms, to the direction of stacking of bilayers of chains,^{78,79} whereas the a_α and c_α axes of the α form and the

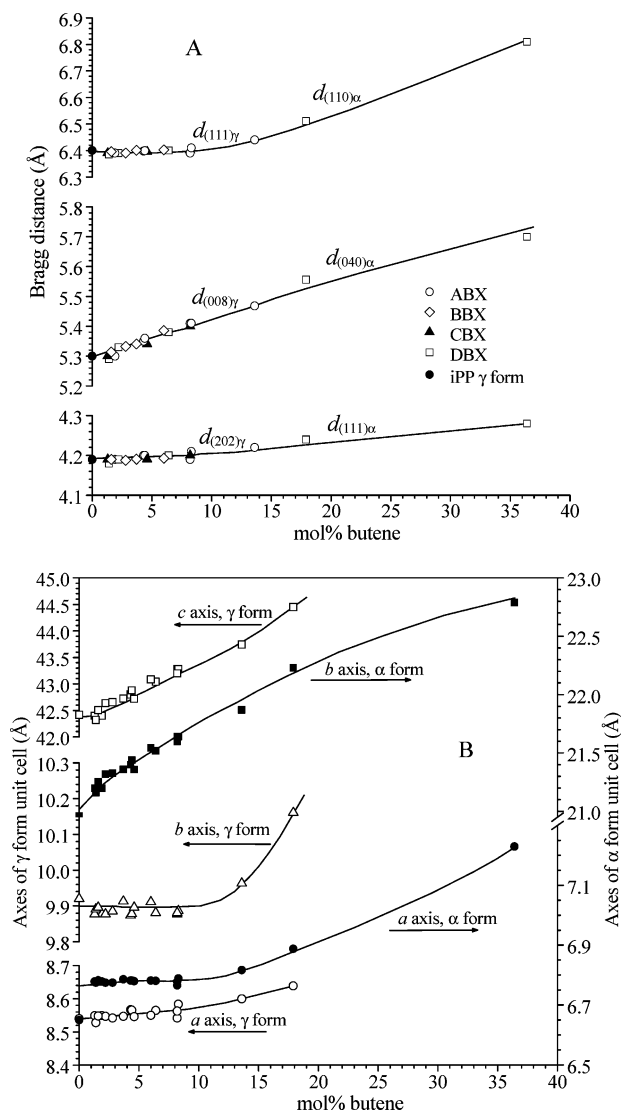


Figure 5. (A) Values of Bragg distances (d) of $(111)_{\gamma}$, $(008)_{\gamma}$, and $(202)_{\gamma}$ reflections of the γ form of iPP and $(110)_{\alpha}$, $(040)_{\alpha}$, and $(111)_{\alpha}$ reflections of the α form of iPP, observed in the X-ray powder diffraction profiles of as-prepared samples of iPPBu copolymers, as a function of butene content. (B) Values of a (\circ), b (Δ), and c (\square) axes of the orthorhombic unit cell of the γ form of iPP, and of a (\bullet) and b (\blacksquare) axes of the monoclinic unit cell of the α form of iPP. The values of Bragg distances of the same reflections and of axes of unit cells of the α and γ forms of iPP homopolymer are also reported at 0% of butene concentration.^{78,79}

a_{γ} and b_{γ} axes of the γ form are nearly constant, at least up to butene concentrations of 10–14 mol % (Figure 5B). We recall that in the orthorhombic unit cell of the γ form the c_{γ} axis does not coincide with the chain axis direction but correspond to the b_{α} axis direction in the crystals of the α form.^{7,9,11,78}

In copolymers with butene concentration higher than 15 mol %, which crystallize basically in the α form, a much larger increase of Bragg distances of $(110)_{\alpha}$ and $(040)_{\alpha}$ reflections and of dimensions of the a_{α} and b_{α} axes of the unit cell of the α form is observed (Figure 5). The values of the a_{γ} , b_{γ} , and c_{γ} axes of the orthorhombic unit cell for crystals of the γ form, and of the a_{α} and b_{α} axes of the monoclinic unit cell for crystals of the α form of iPPBu copolymers are reported in Figure 5B. The values of the chain axis $c_{\alpha} = 6.5$ Å and of $\beta_{\alpha} = 99.3^{\circ}$ of the monoclinic unit cell of the α form of iPP⁷⁹ have been assumed to be constant with the butene content.

This assumption is in agreement with the fact that the values of the a_{γ} and b_{γ} axes of the γ form, which are related to the

periodicity of iPP chains along the chain axis, are nearly constant up to butene concentration of 10–14 mol %. In fact, since in the γ form the chains are oriented along the diagonals of the ab face of the unit cell,⁷⁸ the periodicity of iPP chains along the chain axis (c_{α} axis for the α form) corresponds in the crystals of the γ form to $D = 1/2 \sqrt{\langle a_{\gamma} \rangle^2 + \langle b_{\gamma} \rangle^2} = 6.54$ Å, with $\langle a_{\gamma} \rangle = 8.55$ Å and $\langle b_{\gamma} \rangle = 9.9$ Å, the average values of the a_{γ} and b_{γ} axes of the γ form crystals for iPPBu copolymers with butene concentration up to 14 mol %, whereas the angles between the diagonals corresponds on average to 99° .

The data of Figure 5B allow explaining the experimental evidence that iPPBu copolymers tend to crystallize in the γ form at low butene content, up to 14–15 mol % (Figure 1C–F), and in the α form at higher concentrations (Figure 1F), the maximum amount of the γ form being achieved at butene concentration of 13–14 mol % (Figure 2C,D). In fact, since the 3/1 helical conformation is not disturbed by the presence of butene and the c_{α} axis of the α form is basically constant at 6.5 Å, and at low butene concentrations, up to 14–15 mol %, the a_{α} axis of the unit cell of the α form is nearly constant with butene content, the dimensional equivalence of the a and c axes, typical of crystals of the α form of iPP ($a_{\alpha} = 6.65$ Å, $c_{\alpha} = 6.5$ Å),⁷⁹ is maintained also in iPPBu copolymers up to a butene concentration of 14–15 mol %. This equivalence is the basis for the crystallization mechanism of homoepitaxial α -branching of the α form that leads the typical cross-hatched morphology,^{83,84} involving the growth of transverse daughter lamellae on mother lamellae of the α form and nearly perpendicular orientation of chain axes, with a and c axes of daughter lamellae oriented parallel to the c and a axes, respectively, of the parent one.^{83,84} This packing scheme of isochiral layers occurs in the α form as a local accident, linked with a “stumble” in the alternation of helical hands. In the orthorhombic γ phase this packing of isochiral layers becomes systematic, and generates a bilayer structure with perpendicular orientation of chains at molecular level.⁷⁸ Moreover, γ form can branch on the α phase through the same mechanism of homoepitaxy.⁸⁵ It has been, indeed, shown that when iPP crystallize as mixtures of the α and γ forms, crystals of the γ form can epitaxially crystallize on the lateral (010) growth faces of the α form mother lamellae,⁸⁵ and even when very high amount of the γ form are evidenced by X-ray diffraction, crystals of the γ form are probably nucleated over the preformed crystals of the α form,^{18,85} and the crystallization rates of the α and γ forms become virtually identical.^{48–50}

The α phase lamellar branching and/or the epitaxial deposition of the γ phase on parent γ or α forms are possible thanks to the dimensional equivalence of the a_{α} and c_{α} axes of the α form. In iPPBu copolymers with low butene content, up to 14–15 mol %, the inclusion of butene units in the crystals produces only expansion of b_{α} axis of the α form (or the c_{γ} axis of the γ form), whereas the a_{α} and c_{α} axes of the α crystals remain nearly constant (Figure 5B). Therefore, at these butene concentrations the dimensional equivalence of the a_{α} and c_{α} axes of the α form is preserved and iPPBu copolymers probably crystallize as iPP homopolymer, giving α phase lamellar branching and/or epitaxial deposition of the γ phase on parent γ or α forms. This mechanism allows and favors crystallization of the γ form when the microstructure of the chains, as with the presence of butene defects, tends to induce crystallization of the γ form.

In iPPBu copolymers with butene concentration higher than 15 mol % the inclusion of butene in the crystals of iPP produces a stronger increase of both the a_{α} and b_{α} axes dimensions of

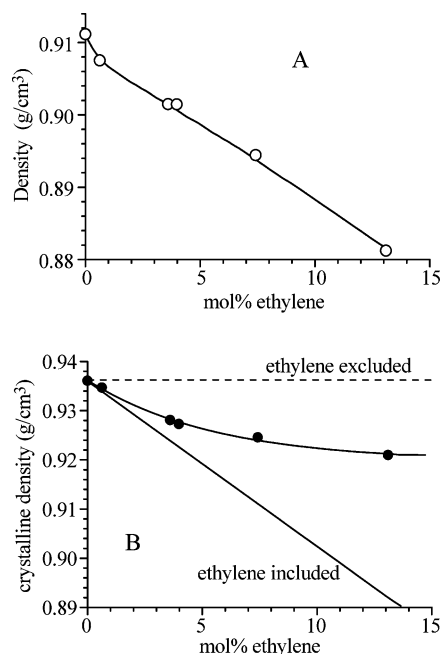


Figure 6. Values of experimental density (A) and of density of the crystalline phase (B) of samples of copolymers iPPet, as a function of ethylene concentration. In B the experimental densities of crystals of copolymers iPPet are compared with the theoretical densities of crystals of the α form calculated assuming complete inclusion of ethylene units in the crystals and complete exclusion from crystals (dashed line, the density of crystals is constant at the value of iPP, $\rho_c = 0.936$ g/cm³).

the α form (Figure 5B). Since the chain axis remains constant at 6.5 Å, the dimensional equivalence of the a_α and c_α axes of the α form is lost and the mechanism of homoepitaxy and epitaxial crystallization of the γ form on crystals of the α form becomes less probable. As a consequence, these iPPBu copolymers crystallize mainly in the α form (Figure 1F) and for butene concentration higher than 25–30 mol % crystallize in the pure α form (profile f of Figure 1F).

Ethylene comonomeric units are also included in crystals of iPPet copolymers, as proved by measurements of the density of the crystalline phase. The values of the experimental density of the semicrystalline iPPet samples, measured by flotation on compression-molded films, are reported in Figure 6A. The density decreases with increasing ethylene concentration, according to the decrease of crystallinity (Figure 4A). The values of density of the crystalline phase of copolymers iPPet are reported in Figure 6B. These values have been evaluated from the experimental density of Figure 6A and the values of crystallinity and density of the amorphous phase. The value $\rho_a = 0.854$ g/cm³ of the density of the amorphous iPP⁸⁶ has been assumed for the density of the amorphous phases of iPPet samples. The experimental density of crystals decreases with increasing ethylene concentration (Figure 6B). Since the volume of the unit cell does not change with increasing ethylene units, the decrease of crystalline density indicates inclusion of smaller ethylene units in the crystals. This is confirmed in Figure 6B by comparing the experimental crystalline density with the theoretical density of the α form crystals, calculated by assuming complete inclusion of ethylene units in the crystals or total exclusion. It is apparent that the experimental crystalline densities are intermediate between the calculated ones, indicating that the ethylene units are only in part included in the crystals of iPPet copolymers and, as already demonstrated in the literature,^{47,48,56} are partitioned between crystalline and amorphous phases.

Crystallization from the Melt. The X-ray powder diffraction profiles of some samples of copolymers isothermally crystallized from the melt are reported in Figure 7. The diffraction profiles of the as-prepared samples are also reported in Figure 7 (profiles a) for comparison. All samples crystallize from the melt as mixtures of the α and γ forms as indicated by the presence in the diffraction profiles of Figure 7 of both $(130)_\alpha$ and $(117)_\gamma$ reflections at $2\theta \approx 18.6$ and 20° of the α and γ forms, respectively. For each sample, the fraction of the γ form increases with increasing crystallization temperature, as indicated by the increase of the $(117)_\gamma$ reflection of the γ form with increasing crystallization temperature in the diffraction profiles of Figure 7. Moreover, for both iPPet and iPPBu copolymers the amount of the γ form generally increases with increasing concentration of comonomeric units (Figure 7B,C and Figure 7D,E). In the case of iPPBu copolymers, as already observed for the as-prepared samples, the amount of the γ form in melt-crystallized samples decreases for butene concentrations higher than 14–15 mol % (compare Figure 7H, I and L) and samples with butene contents higher than 25–30 mol % crystallize from the melt exclusively into α form at any crystallization temperature (Figure 7L). Samples of iPPet copolymers with ethylene concentration higher than 10 mol %, instead, crystallize from the melt in the γ form at every crystallization temperature (Figure 7C), although disordered modifications of the γ form are always obtained, as indicated by the low intensity of the $(117)_\gamma$ reflection at $2\theta = 20.1^\circ$ in the X-ray diffraction profiles of Figure 7C.

The comparison of X-ray diffraction profiles of iPPBu and iPPet samples containing similar concentrations of comonomeric units and prepared with the same catalyst, therefore containing similar concentration of stereodeflects (for instance samples of Figure 7, parts A and D), clearly indicates that a much higher concentration of the γ form is obtained in the melt-crystallized samples of iPPet copolymers.

Moreover, samples of iPPBu copolymers crystallize from the melt in more ordered modifications of the γ form (at low butene concentration, up to 10–14 mol %) and α form (at butene contents higher than 15 mol %), as indicated by the sharpness and high intensities of $(117)_\gamma$ and $(130)_\alpha$ reflections at $2\theta \approx 20$ and 18° of the γ and α forms respectively, in the diffraction profiles of Figure 7D–L (see also the thermal analysis reported in the Supporting Information). Furthermore, as discussed for as-prepared samples, melt-crystallized samples of iPPBu copolymers show values of crystallinities higher than those of iPPet copolymers having similar concentrations of comonomeric units and stereodeflects.

Finally, for both iPPet and iPPBu copolymers, the comparison of diffraction profiles of samples prepared with different catalysts containing different concentration of *rr* stereodeflects but similar concentration of comonomeric units (for instance compare Figure 7, parts A and B, or Figure 7, parts D, F, and G), indicate that more stereoirregular samples, containing higher concentrations of *rr* stereodeflects, develop a higher amount of the γ form.

The values of relative amount of the γ form with respect to the α form, f_γ , in the various samples of iPPet and iPPBu copolymers, evaluated from the intensities of $(117)_\gamma$ and $(130)_\alpha$ reflections in the diffraction profiles of Figure 7, are reported in Figure 8 as a function of the crystallization temperature. Data of the amount of the γ form for iPP samples of Table 1, prepared with the same catalysts, which were already reported in the literature,^{12,17} are also reported in Figure 8 for comparison. As already observed in the literature for stereoirregular samples

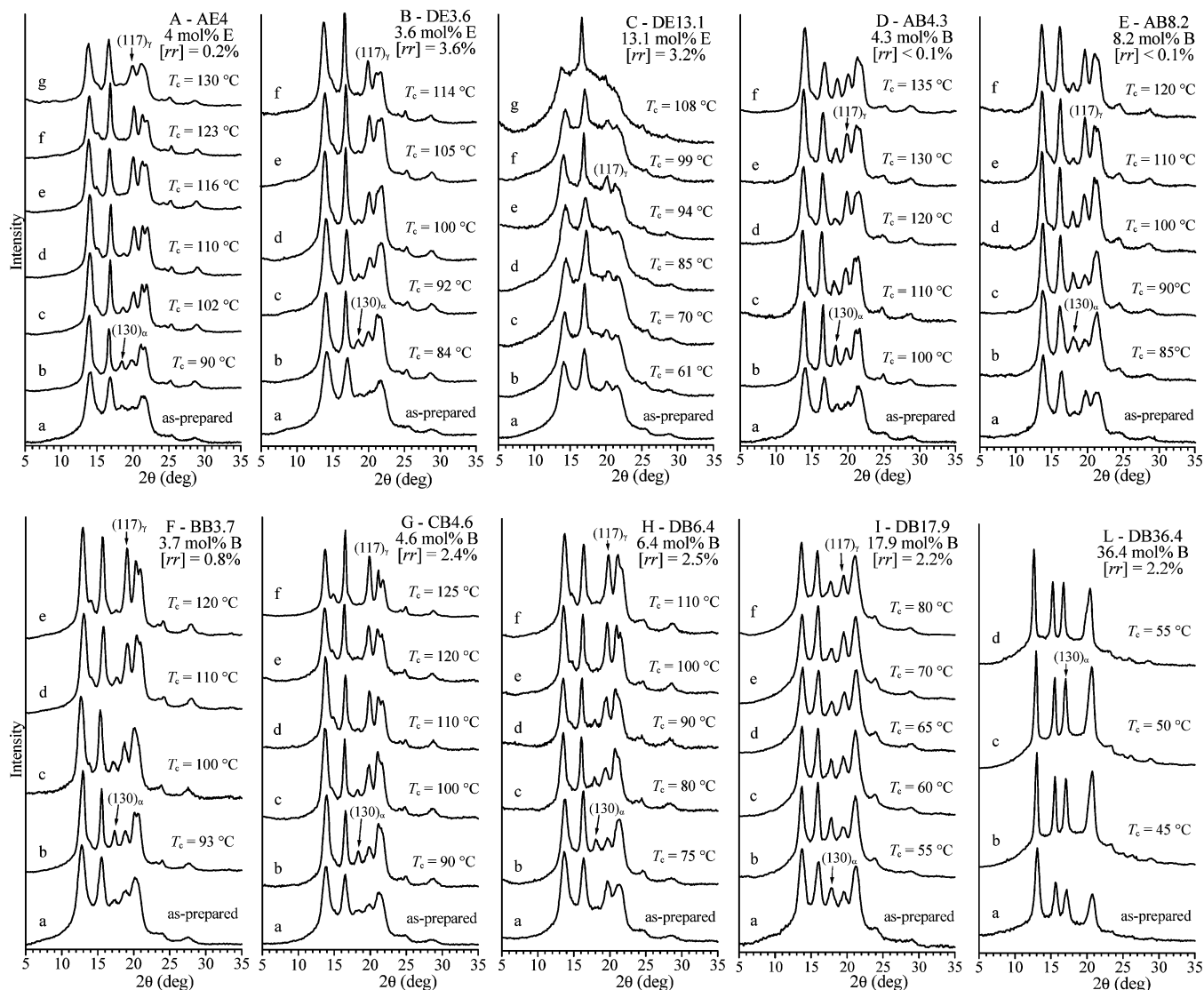


Figure 7. X-ray powder diffraction profiles of some samples of iPPet and iPPBu copolymers isothermally crystallized from the melt at the indicated crystallization temperature T_c . The $(130)_\alpha$ reflection of the α form at $2\theta \approx 18.6^\circ$ and the $(117)_\gamma$ reflection of the γ form at $2\theta \approx 20^\circ$ are indicated. The concentrations (mol %) of ethylene (E) and butene (B) units are also indicated. The diffraction profiles of as-prepared sample (profiles a) are also reported for comparison.

of iPP homopolymer^{1–3,6,8–10,12–15,17} and for iPP-based copolymers,^{27c,30,42–44,48–50,65} for each sample the content of the γ form increases with increasing crystallization temperature, and a maximum amount of the γ form is obtained at different crystallization temperatures. Moreover, the amount of the γ form generally increases with increasing concentration of comonomeric units (Figure 8). For samples of iPPet and iPPBu copolymers prepared with catalyst **A** (Figure 8A and C), containing a very small concentration of stereo- and regiodefects, the much higher amount of the γ form than that observed for the homopolymer sample iPPA, containing similar or slightly higher concentrations of *rr* and 2,1 defects (Tables 1–3), is exclusively due to the presence of ethylene and butene units.

The data of Figure 8A and C clearly indicate that, while for iPPet copolymers the maximum fraction of the γ form increases with increasing ethylene concentration and achieves the value of $f_\gamma = 1$ already for ethylene content of 4 mol % (Figure 8A), in the case of iPPBu copolymers the amount of the γ form achieves a maximum value for samples with butene concentrations of nearly 8 mol % and then decreases for higher butene concentrations (compare samples with 8 and 13.6 mol % of butene units in Figure 8C). Since in these samples the

concentrations of *stereo*- and *regio*-defects are very small and nearly the same ($[rr] + [2,1e] \approx 0.2–0.9\%$), this different behavior is only due to the different influence of ethylene and butene units on the crystallization of the α and γ forms.

In both iPPet and iPPBu copolymers, samples prepared with less stereospecific catalysts **B**, **C**, and **D**, containing higher amounts of *rr* stereodefects (0.7–1%, 1.9–2.4%, and 2.2–3.4 mol %, respectively, for iPPBu copolymers), develop by melt-crystallization higher concentrations of the γ form than those obtained for samples prepared with the catalyst **A** (compare Figure 8, parts A and B, for iPPet copolymers and Figure 8C–F for iPPBu samples). The effect of *rr* defects is clearly shown in Figure 9A where the fractions of the γ form in iPPBu samples prepared with different catalysts containing different concentrations of *rr* defects and similar amounts of butene units are compared. It is apparent that the higher the concentration of *rr* defects, the higher the fraction of the γ form crystallized from the melt. The two effects of the presence *rr* stereodefects and of comonomeric units in inducing crystallization of the γ form are added, and stereoirregular iPPet and iPPBu copolymers containing high concentration of *rr* defects and comonomeric

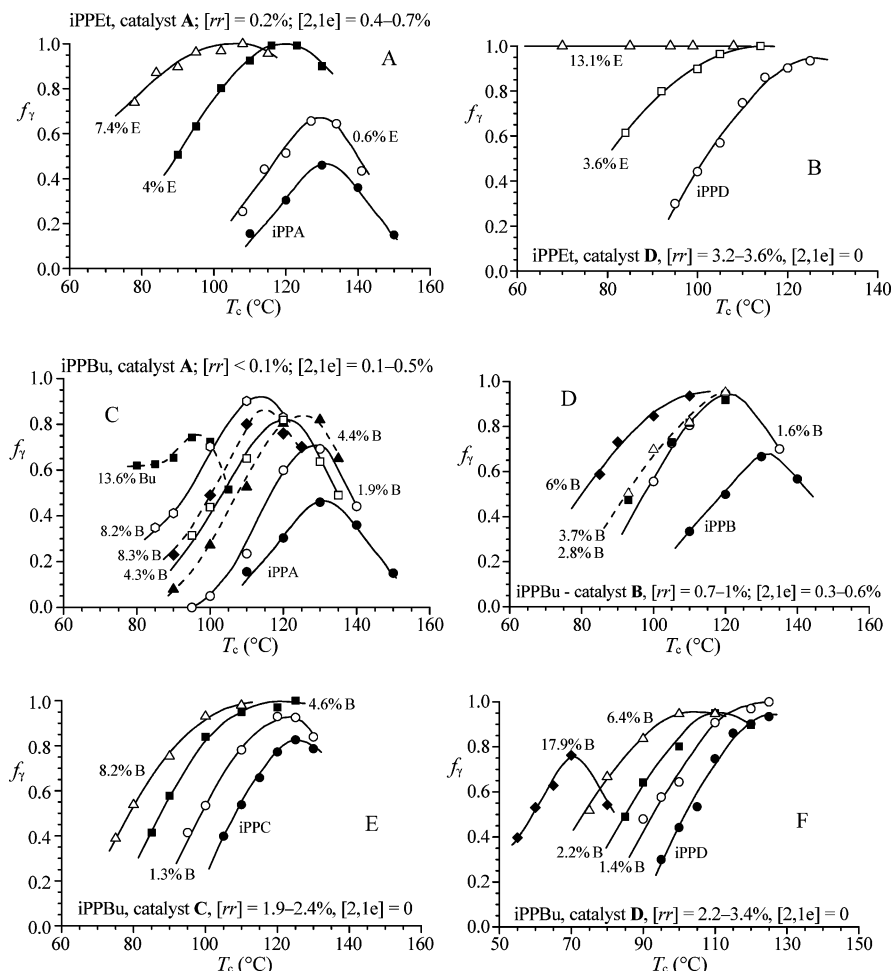


Figure 8. Relative amount of the γ form of iPP, f_γ , with respect to the α form, evaluated from the X-ray diffraction profiles of Figure 7, in samples of iPPet copolymers prepared with catalysts **A** (A) and **D** (B) and iPPBu copolymers prepared with catalysts **A** (C), **B** (D), **C** (E), and **D** (F), isothermally crystallized from the melt, as a function of the crystallization temperature T_c . Data of f_γ for the four samples of iPP homopolymers iPPA, iPPB, iPPC, and iPPD, prepared with the same catalysts, are also reported. The concentrations (mol %) of ethylene (E) and butene (B) units are indicated.

units crystallize basically in the pure γ form (Figure 8B and Figure 8E,F).

Also for stereoirregular samples prepared with catalyst **D**, iPPBu copolymers present a peculiar behavior (Figure 8F). A maximum concentration of the γ form is achieved already at low butene contents (2–6 mol %), favored by the presence of high concentrations of rr defects (3.4 mol %), then the maximum amount of the γ form decreases in samples containing high concentration of butene units (sample with 17.9, mol % of butene, Figures 7I and 8F), and samples with butene contents higher than 30 mol % crystallize from the melt exclusively into α form at any crystallization temperature (sample DB36.4 of Figure 7L).

In particular, Figure 8F clearly shows that the maximum amount of the γ form achieved for the homopolymer sample iPPD, prepared with catalyst **D**, is much higher than that obtained for the iPPBu copolymer sample having 17.9 mol % of butene units. The presence of high concentration of rr defects (3.5 mol %) induces crystallization of the γ form in the homopolymer sample, whereas the additional presence of very high concentration of butene units in the sample DB17.9, higher than 10–14 mol %, favors crystallization of the α form, notwithstanding the presence of stereodefects (2.2 mol %). This indicates that rr defects and butene units exert a different influence on the crystallization of the α and γ forms of iPP.

This unexpected behavior is not observed in iPPet copolymers where rr defects and ethylene units seem to give a similar

influence in favoring crystallization of the γ form. The effect of ethylene units is added to that of rr stereodefects and stereoirregular samples also containing high ethylene concentration crystallize from the melt in the pure γ form (Figure 8B).

The different behavior of ethylene and butene units is shown in Figure 9, parts B and C, where the fractions of the γ form that develop in iPPet and iPPBu copolymers having similar concentrations of comonomeric units and of rr stereodefects and 2,1e regiodefects are compared. In the case of highly stereoregular samples prepared with the catalyst **A**, containing very small amounts of rr defects (Figure 9B), iPPet copolymer samples always present much higher content of the γ form than iPPBu copolymers of similar comonomer concentrations. For stereoirregular samples prepared with the catalyst **D**, containing high concentrations of rr defects (2.2–3.4% for iPPBu and 3.2–3.6% for iPPet), at low comonomer concentrations (2–4 mol %) iPPet samples still present higher amounts of the γ form (Figure 9C), but the difference between iPPet and iPPBu is not as high as in the case of more stereoregular samples (Figure 9B). This is due to the fact that when the comonomer concentration is low, the crystallization of both iPPet and iPPBu copolymers is dominated by the presence of the high concentration of rr defects, that induces formation of the γ form. At high comonomer concentrations, the crystallization is, instead, governed by the different effects of ethylene and butene units, so that iPPet copolymers crystallize basically in the pure γ form (sample with 13.1 mol % of ethylene in Figure 9C), whereas

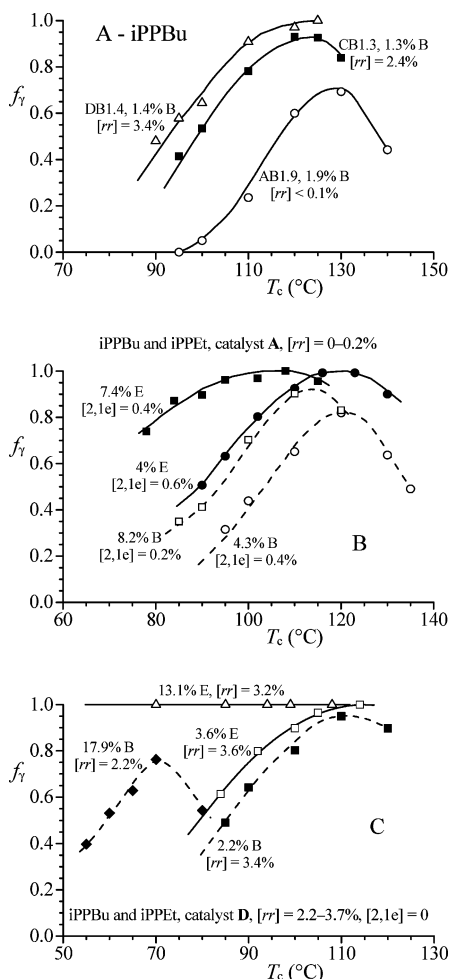


Figure 9. Relative amount of the γ form of iPP, f_γ , evaluated from the X-ray diffraction profiles of Figure 7, in samples of iPPEt and iPPBu copolymers isothermally crystallized from the melt, as a function of the crystallization temperature T_c . (A) Comparison between samples of iPPBu copolymers prepared with catalysts A, C, and D, having similar concentrations of butene units but different concentrations of rr defects ($\approx 0\%$, 2.4% , and 3.4% mol %, respectively). (B) Comparison between samples of iPPEt and iPPBu copolymers prepared with the catalyst A having similar concentration of comonomeric units. (C) Comparison between samples of iPPEt and iPPBu copolymers prepared with the catalyst D having similar concentration of comonomeric units. The concentrations (mol %) of ethylene (E) and butene (B) units are indicated.

iPPBu samples with butene content higher than 15–17 mol % crystallize mostly in the α form (Figure 9C).

As extensively reported in the literature,^{1–3,8,9,12–15,17} the maximum amount of the γ form that crystallizes upon melt-crystallization procedures, depend on the microstructure of iPP chains, that is, on type and concentration of defects and molecular mass.¹⁷

The values of the maximum amount of the γ form ($f_\gamma(\text{max})$) that develop by melt-crystallizations of iPPEt and iPPBu copolymers, evaluated from the maximum of the curves of Figure 8, are reported in Figure 10 as a function of ethylene and butene concentrations (Figure 10A,C) and of the total concentration of defects $\epsilon = [rr] + [2,1e] + [\text{comonomer}]$ (Figure 10B,D). It is apparent that, while for iPPEt copolymers the value of $f_\gamma(\text{max})$ increases with increasing ethylene concentration up to achieve the maximum value $f_\gamma(\text{max}) = 1$ that remain constant for all ethylene concentrations compatible with the crystallization (Figure 10A), for iPPBu copolymers, $f_\gamma(\text{max})$ first increases, achieves a nearly constant maximum value and

then decreases with increasing butene content (Figure 10C). Moreover, in both iPPEt and iPPBu copolymers (and also for the corresponding iPP homopolymers prepared with the same catalysts) the value of $f_\gamma(\text{max})$ increases with increasing concentration of rr defects (Figure 10, parts A and C).

However, in the case of iPPEt copolymers, the data of $f_\gamma(\text{max})$ as a function of the total concentration of defects ($\epsilon = [rr] + [2,1e] + [\text{ethylene}]$) are fitted by a single curve (Figure 10B), indicating that rr stereodefects and ethylene comonomeric units exert similar effects in inducing crystallization of the γ form. The two effects are added, and samples containing the same total concentration of defects give the same maximum amount of the γ form regardless of stereoregularity and ethylene concentration. Samples of iPPBu copolymers having the same total concentration of defect ϵ give, instead, different maximum amounts of the γ form (Figure 10D). In particular, more stereoirregular samples containing higher content of rr defects (samples DBX with $[rr] = 2.2\text{--}3.4\%$), give values of $f_\gamma(\text{max})$ higher than those of more stereoregular samples with similar values of ϵ , containing lower amounts of rr defects but higher concentrations of butene (for instance samples ABX with $[rr] < 0.1\%$). This indicates that rr stereodefects and butene comonomeric units exert different effects in inducing crystallization of the γ form.

The comparison of iPPEt and iPPBu copolymers, shown in Figure 10D, clearly indicates that iPPBu copolymers always produce lower values of the maximum amount of the γ form. Only in the case of stereoirregular samples containing high concentration of rr defects ($2.0\text{--}3.4\%$) prepared with catalysts C and D do iPPEt and iPPBu copolymers give similar values of $f_\gamma(\text{max})$, at least for total concentrations of defects up to $\epsilon = 10\text{--}14\text{ mol } \%$ (Figure 10D). This is due to the fact that in these samples the crystallization is mainly governed by the presence of high concentration of rr defects that induce formation of the maximum amount of the γ form.

The data of Figure 10 indicate that the effects of different types of defects on the polymorphic behavior of iPP are different. Ethylene units and rr stereodefects produce a more efficient effect in inducing crystallization of the γ form than that of butene units. The role of the defects is, therefore, not just limited to the effect of shortening the length of regular fully isotactic sequences.

However, all data reported in the literature so far agree with the hypothesis that the crystallization of the γ form is favored when the regular isotactic sequences are short^{1–3,6,8–15,17,21} and, therefore, when the total concentration of any type of defects is high and no differences have been observed for different kinds of defects. However, only in the case of iPP copolymers, Alamo et al.⁴⁸ have observed that ethylene, butene, hexene, and octene comonomeric units produce different values of the regular isotactic crystallizable propylene sequences because of the different degree of inclusion of comonomers in the crystalline lattice. Comonomers rejected from the crystals would produce shorter crystallizable sequences and higher concentration of the γ phase.⁴⁸ However, also from these literature data there is no discrimination of defects that enter the crystal lattice (*stereo-* or *regio*defects, or comonomeric units) between crystals of the α or γ forms. This is the key to discriminating the role of different defects.

For metallocene-made iPP homopolymer samples and iPP-based copolymers the distribution of defects (stereodefects and comonomeric units) along the polymer chains is random; hence, the values of the average length of the fully isotactic propylene sequences, $\langle L_{iPP} \rangle$, have been evaluated as inversely proportional

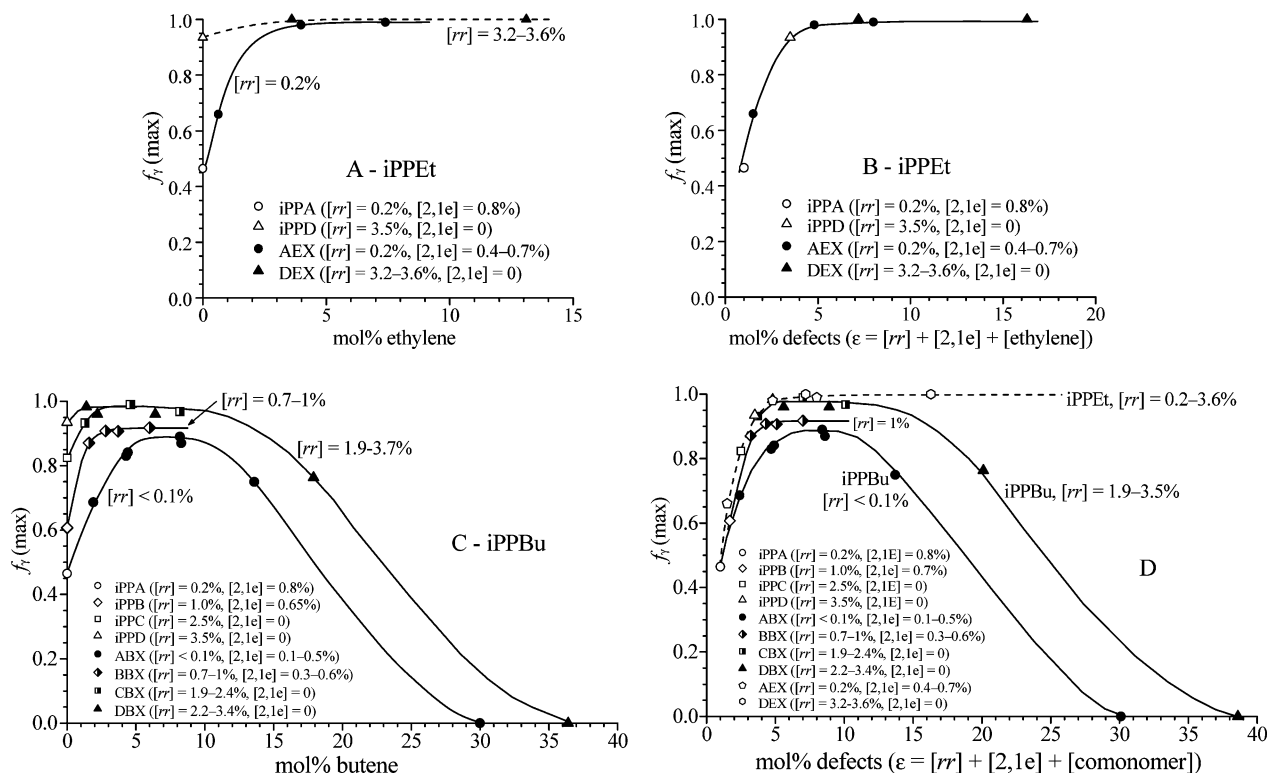


Figure 10. Maximum amount of the γ form ($f_\gamma(\text{max})$) as a function of concentration of ethylene (A) and butene units (C) and of total concentration of defects ($\epsilon = [rr] + [2,1e] + [\text{comonomer}]$) (B,D) obtained in iPPeT (A,B) and iPPBu (B,D) copolymers crystallized from the melt.

to the total content of microstructural defects. Only recently we have been able to analyze the single effect of rr stereodefects on the crystallization of the γ and α forms of iPP thanks to the structural studies of iPP homopolymer samples characterized by a very simple microstructure, containing largely one type of defects (isolated rr triads) in a wide range of concentration and free from any other microstructural defects.¹² This allowed us to find a precise relationship between the maximum amount of the γ form and the average length of the fully isotactic sequences from the ^{13}C NMR data as $\langle L_{iPP} \rangle = (2[mm]/[mr]) + 2$. This relationship is reported in Figure 11 in a logarithmic scale of $\langle L_{iPP} \rangle$ to amplify the region corresponding to very small values of $\langle L_{iPP} \rangle$ and high concentration of defects. For iPPeT and iPPBu copolymers, containing rr stereodefects, 2,1 regiodefects, and comonomers, the average length of regular isotactic polypropylene sequences can be roughly evaluated as $\langle L_{iPP} \rangle = 1/\epsilon$, where $\epsilon = [rr] + [2,1e] + [\text{comonomer}]$ is the total concentration of defects (Tables 1–3). The values of maximum amount of the γ form, $f_\gamma(\text{max})$, obtained for iPPeT and iPPBu copolymers and corresponding homopolymers iPPA–iPPD from the data of Figures 8 and 10, are reported in Figure 11 as a function of the average length of the fully isotactic polypropylene sequences $\langle L_{iPP} \rangle$ and are compared with the relationship found for iPP homopolymer samples.¹²

It is apparent that the data of $f_\gamma(\text{max})$ obtained for the samples iPPA and iPPB containing 2,1 regiodefects are well-interpolated on the relationship obtained in ref 12 with the iPP samples containing only rr stereodefects (including the samples iPPC and iPPD).¹⁷ As already shown in ref 17, this indicates that rr stereodefects and 2,1e regiodefects give a similar effect of reducing the length of regular isotactic sequences, at least for low concentration of defects (in the range 1–3%), and give the same influence on the crystallization of the γ form.

Moreover, Figure 11 clearly indicates that the data of $f_\gamma(\text{max})$ obtained for all iPPeT copolymers (samples AEX and DEX)

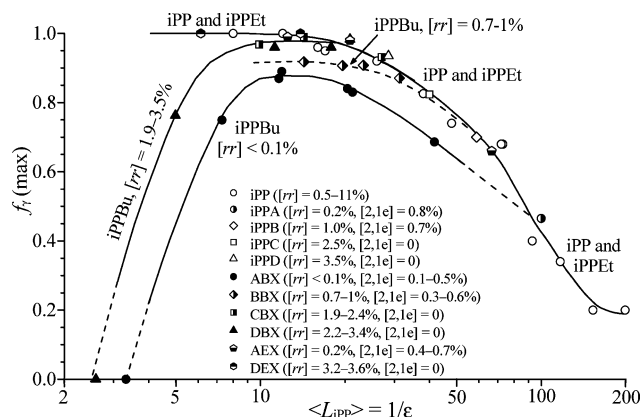


Figure 11. Maximum amount of the γ form, $f_\gamma(\text{max})$, crystallized by isothermal crystallizations from the melt, evaluated from the maxima of the curves of Figure 8, as a function of the average length of fully isotactic propylene sequences $\langle L_{iPP} \rangle$, for samples of iPPBu copolymers prepared with catalysts **A** with $[rr] < 0.1\%$ (●), **B** with $[rr] = 0.7-1\%$ (tilted square, half solid), **C** with $[rr] = 1.9-2.4\%$ (■) and **D** with $[rr] = 2.2-3.4\%$ (▲) and of iPPeT copolymers prepared with the catalysts **A** with $[rr] = 0.2\%$ (pentagon, half solid) and **D** with $[rr] = 3.2-3.6\%$ (hexagon, half solid), and corresponding iPP homopolymer samples iPPA (●), iPPB (◇), iPPC (□), and iPPD (△), prepared with the same catalysts. The average length of fully isotactic propylene sequences has been evaluated as $\langle L_{iPP} \rangle = 1/\epsilon$, where ϵ is the total concentration of defects $\epsilon = [rr] + [2,1e] + [\text{comonomer}]$. The data of the copolymers are compared with the relationship between $f_\gamma(\text{max})$ and $\langle L_{iPP} \rangle$ found in ref 12 for samples of iPP homopolymer of different stereoregularity, characterized by the presence of variable amount of rr stereodefects (○). For these samples the values of $\langle L_{iPP} \rangle$ have been evaluated from the ^{13}C NMR data,¹² as $\langle L_{iPP} \rangle = (2[mm]/[mr]) + 2$.

are also well-interpolated by the same curve corresponding to the data of the stereoirregular iPP samples containing only rr stereodefects. This confirms that ethylene comonomeric units behave as rr stereodefects at any concentration. They exert a similar effect on the crystallization of iPP. Both ethylene units and rr stereodefects produce a shortening of the regular fully

isotactic PP sequences inducing crystallization of the γ form. Samples of iPP homopolymers containing only rr defects and iPPEt copolymers characterized by the same value of $\langle L_{iPP} \rangle$ give the same maximum amount of the γ form, regardless of the relative concentration of rr and ethylene units. At high defect concentration (ϵ higher than 5–7 mol %) and low average length of iPP sequences ($\langle L_{iPP} \rangle$ lower than 15–20 monomeric units) crystallization of the pure γ form is observed in both iPP homopolymer¹² and iPPEt copolymer samples.

The data of $f_{\gamma}(\max)$ for samples of iPPBu copolymer are, instead, not fitted by the master curve corresponding to the data of the stereoirregular iPP homopolymer and iPPEt copolymer samples (Figure 11) and different relationships between $f_{\gamma}(\max)$ and $\langle L_{iPP} \rangle$ are obtained depending on the stereoregularity. Only for very low concentration of butene units and high values of $\langle L_{iPP} \rangle$ the data of iPPBu copolymers converge on the master curve of stereodeficient iPPs (Figure 11). Moreover, samples of iPPBu copolymers characterized by the same value of the average length of iPP sequences (having the same total concentration of defect ϵ) give different maximum amount of the γ form depending on the concentration of rr defects (Figure 11). In particular, at the same value of $\langle L_{iPP} \rangle$, more stereoirregular samples containing higher content of rr defects (samples CBX and DBX with $[rr] = 1.9$ –2.4% and 2.2–3.4%, respectively), give values of $f_{\gamma}(\max)$ higher than those of more stereoregular samples containing lower rr content (for instance samples ABX and BBX with $[rr] < 0.1\%$ and $[rr] = 0.7$ –1.0%, respectively). iPPBu copolymers always produce values of maximum amount of the γ form lower than those obtained for stereodeficient iPP homopolymers and iPPEt copolymers samples having the same value of $\langle L_{iPP} \rangle$. This indicates that the effect of butene units on the crystallization of the γ form is completely different from that of rr stereodeficient and ethylene units. The single effect of butene units is given in Figure 11 by the curve corresponding to iPPBu samples containing negligible amount of rr defects (samples ABX with $[rr] < 0.1\%$). Only in the case of stereoirregular samples containing high concentration of rr defects (2.0–3.4%) prepared with catalysts **C** and **D**, iPPBu copolymers give values of $f_{\gamma}(\max)$ similar to those of iPPEt copolymers and stereodeficient iPP samples, at least for total concentration of defects lower than 5–7 mol % and values of $\langle L_{iPP} \rangle$ higher than 15–20 monomeric units (Figure 11). This is due to the fact that in these samples the crystallization is mainly governed by the presence of high concentration of rr defects that induce formation of the maximum amount of the γ form.

Finally, Figure 11 shows that for iPPBu copolymers, the values of $f_{\gamma}(\max)$ decrease for very low values of $\langle L_{iPP} \rangle$ (lower than 10 monomeric units, corresponding to concentration of butene units, or total concentration of defects, higher than 10 mol %) and these samples tend to crystallize in the α form. The result that the crystallization of the α form is favored for very short values of the average length of the regular propylene sequences $\langle L_{iPP} \rangle$ is reported here for the first time and is opposite to what has been generally accepted so far that short regular propylene sequences favor crystallization of the γ form.^{1–3,6,8–15,17,21} For stereodeficient iPP homopolymer and iPPEt copolymer samples, instead, the maximum amount of the γ form achieves the maximum value $f_{\gamma}(\max) = 1$ for values of $\langle L_{iPP} \rangle = 20$ –30 monomeric units, and this remains constant for all concentrations of rr defects or ethylene units compatible with the crystallization.

These data indicate that the crystallization of the γ form of iPP is not just related to the value of the average length of the regular fully isotactic propylene sequences $\langle L_{iPP} \rangle$. Microstructural defects or comonomeric units act as interruption of the regular iPP sequences but their role is not only limited to shorten the

regular isotactic sequences. The different behavior of rr stereodeficient and ethylene and butene comonomeric units may be related to the inclusion of stereodeficient and constitutional defects in the crystals of the α and γ forms of iPP and the different compatibility of the different defects within the crystalline lattices of the different polymorphic forms of iPP, which produces a difference in the partitioning of defects between crystals of the α and γ forms.

The results of Figures 3–6 and all data reported in the literature,^{41,44,48,56,65} namely the higher degree of crystallinity of iPPBu copolymers compared with that of iPPEt samples (Figure 4A), support the hypothesis that the degree of inclusion of ethylene is much lower than that of butene. Because of the inclusion of defects, the length of the crystallizable sequences is much longer than the value of $\langle L_{iPP} \rangle$ of Figure 11.

It has been recently suggested that defects of stereoregularity, such as isolated rr triads, can be more easily tolerated at low cost of conformational and packing energy in the crystal lattices of the γ form and of the α/γ disordered modifications.^{7,9,11} Low conformational energy models of iPP chains containing rr defects, proposed in ref 7, are shown in Figure 12A,B. In the model of Figure 12B, the presence of rr defects produces inversion of the chirality of the 3-fold helix and a bending of the chain.⁷ Calculations of the packing energy have indicated that this bent defective chain could be accommodated in the lattices of the γ form and α/γ disordered modifications of iPP but not in the lattice of the α form.^{7,11} In the low-energy model of Figure 12A, the chain stems connected by the punctual rr defect have the same chirality and maintain the same axis. The resulting chain is straight and could be easily accommodated in crystals of both α and γ forms, the values of the packing energy being very similar for α and γ lattices. This suggests that rr defects are possibly included in both α and γ form crystals, but the inclusion in the γ form is more probable because the bent conformation of Figure 12B is of the lowest energy and compatible only with the crystalline lattice of the γ form.

Similar calculations of conformational and packing energies have been performed for iPP chains containing ethylene and butene comonomeric units. The results of the modeling are shown in Figure 12C–F. Ethylene units behave as rr stereodeficient, that is, the two low conformational energy models of Figure 12, parts C and D, with parallel and bent chain stems connected by the ethylene defect, respectively, suitable for the packing in crystals of the α form and the γ form, respectively, are isoenergetic. Therefore, ethylene units may produce inversion of the chirality of the 3-fold helix and a bending of the chain or a straight chain that maintains the same chirality before and after the defect. Packing energy calculations have shown that the bent conformations of Figure 12D having helical stems with opposite chirality connected by the defect can be easily accommodated only in crystals of the γ form or in α/γ disordered modifications, but not in the α form, whereas the model of Figure 12C can be accommodated in crystals of both the α and γ forms. This suggests that, as in the case of rr defects, ethylene units may be included in crystals of the α and γ forms, but inclusion in the γ form or in the α/γ disordered modifications is more probable.

In the case of iPP chains containing butene units as defects, only models of straight chain of Figure 12, parts E and F, with the chain stems connected by the butene defect having the same chirality and parallel axes, have low conformational energy. Models of bent chains with helix reversal are, indeed, of high energy. Packing energy calculations have shown that the modeled chains of iPP containing butene defects (Figure 12E,F)

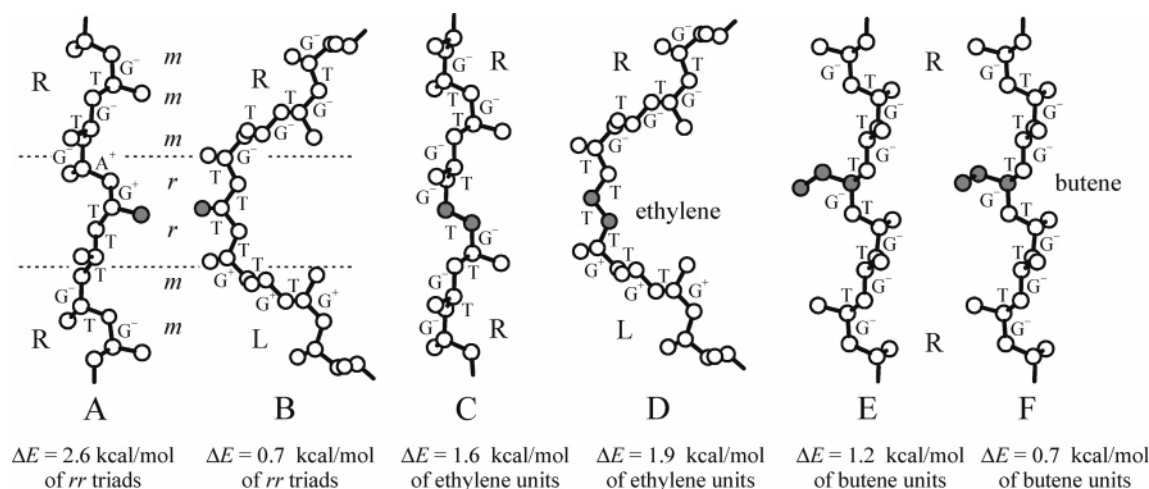


Figure 12. Minimum energy conformations of iPP chains in 3/1 helical conformation containing isolated *rr* triads (A, B), ethylene (C, D) and butene (E, F) defects. The values of backbone dihedral angles ($T \approx 180^\circ$, $G \approx \pm 60^\circ$, $A \approx 120^\circ$) and the chirality of the chain branches above and below the defects (R = right-handed, L = left-handed) are indicated. The minimum energy conformation of chains containing an isolated *rr* stereodeflect (A) emulates the shape of a fully isotactic iPP chain and is close to that one shown in Figure 5 of ref 5, found using a simulated annealing procedure. For chains containing isolated butene units (E, F), low energy conformations correspond to small deviations of the backbone dihedral angles from the trans (T) and gauche (G) values. The pendant methyl group of the butene unit is in *trans* conformation with respect to one adjacent backbone methylene carbon atom and in *gauche* conformation with respect to the second adjacent methylene group in model E, whereas it is in *gauche* conformation with respect to both adjacent backbone methylene groups in model F. The conformational energy of each defect is given with respect to the energy of a defect-free model chain of iPP in 3/1 helical conformation. The atoms of the monomeric unit corresponding to the defect (*rr* triad, ethylene and butene) are indicated as gray circles.

could be easily accommodated without differentiation in crystals of the α and γ forms.

These results can explain the data of Figure 10 and 11 that have indicated that *rr* stereodeflect and ethylene units favor crystallization of the γ form, whereas high contents of butene units favor crystallization of the α form. This is possibly due to the fact that *rr* stereodeflects and ethylene units are probably more easily included in crystals of the γ form, whereas butene units are included without differentiation in crystals of both α and γ forms, but probably more easily in the α form at high concentrations.

This analysis indicates that the crystallization properties and polymorphic behavior of iPP and corresponding copolymers depend on a double role played by stereodeflects, regiodeflects, and constitutional defects. The first effect is the interruption of the regular fully isotactic propylene sequences with shortening of the average length of the crystallizable sequences $\langle L_{iPP} \rangle$, which favors crystallization of the γ form that does not need for chain folding.⁴⁸ This effect is common to any defects (*stereo*- and *regio*-deflects and comonomeric units) and may be more or less efficient depending on the effective disturbance of the defect, which, in turn, is related, in the case of copolymers, to the size of the comonomeric units.⁴⁸ The second effect is due to the possible inclusion of defects in the crystals of the α and γ forms of iPP. This favors crystallization of the crystalline form that better tolerates the defect within its crystalline lattice. In the case of iPPet and iPPBu copolymers, since different proportions of ethylene and butene units are included in crystals of the α and γ forms, the two effects act simultaneously, and one prevails over the other depending on the compatibility of the different defects within the crystalline lattices of the different polymorphic forms. Ethylene and *rr* stereodeflects are included in crystals of both α and γ forms but are probably more easily included in crystals of the γ form and in α/γ disordered modifications of the γ form. In iPPet copolymers and in stereodeflective iPP samples, the effects of crystal inclusion and of shortening the regular propylene sequences produce the same result of favoring the crystallization of the γ form.

In the case of iPPBu copolymers, butene units are included without differentiation in crystals of the α and γ form, but probably more easily in the α form at high concentrations. At low butene concentration, up to nearly 10 mol %, the effect of shortening the length of regular isotactic propylene sequences prevails and induces crystallization of the γ form. Hence, at high value of $\langle L_{iPP} \rangle$, in the range 10–100 monomeric units, the maximum amount of the γ form increases with increasing butene concentration and decreasing $\langle L_{iPP} \rangle$. For high butene concentrations, higher than 10 mol %, the effect of inclusion of butene units in crystals of the α form, that induce crystallization of the α form, prevails over that of the shortening of $\langle L_{iPP} \rangle$.

In addition the increase of the a_α axis dimension of the α form for butene content higher than 10–15 mol % determines the loosing of dimensional equivalence of the a_α and c_α axes of the α form, so that the mechanism of epitaxial crystallization of the γ form on parent α form lamellae becomes less probable. This produces a decrease of the amount of the γ form for butene concentration higher than 10–15 mol % and $\langle L_{iPP} \rangle$ lower than 10 monomeric units, and a corresponding increase of the amount of the α form that crystallizes from the melt (Figure 11). This is confirmed by the fact that iPPBu samples with butene concentrations higher than 20–30 mol % always crystallize in the pure α form (Figure 7L).

It is worth noting that in both iPPet and iPPBu copolymers the crystallizable sequences are longer than the average length of regular fully isotactic propylene sequences $\langle L_{iPP} \rangle$, because of the inclusion of counits in the crystals. In particular, in the case of iPPBu copolymers, the crystallizable sequences are longer than in iPPet owing to the complete cocrystallization of propylene and butene units.

Conclusions

The crystallization properties and the polymorphic behavior of isotactic propylene–ethylene and propylene–butene copolymers prepared with different metallocene catalysts are analyzed. The precise control of stereoregularity and concentration of comonomers has allowed studying and discriminating the

influence of stereodeflects and ethylene and butene units on the crystallization of the α and γ forms of iPP.

The melting temperature of both iPPet and iPPBu copolymers decreases with increasing comonomer concentration and decreasing stereoregularity. iPPBu copolymers always present melting temperatures and crystallinity higher than those of iPPet copolymers of similar comonomer concentration. This indicates that butene units produce disturbances of the crystallization of iPP lower than those produced by ethylene units, notwithstanding the bigger size, and even lower than those of *rr* stereodeflects.

As-prepared and melt-crystallized samples of iPPet and iPPBu copolymers crystallize as mixtures of the α and γ forms, and the fraction of the γ form increases with increasing concentrations of comonomers, *rr* stereodeflects, and crystallization temperature. iPPBu copolymers always develop an amount of the γ form lower than that in iPPet copolymers. The amount of the γ form decreases for butene content higher than 10 mol %, and samples with butene content higher than 25–30 mol % crystallize exclusively in the α form. These data indicate that *rr* defects and ethylene units exert similar effects in inducing crystallization of the γ form, whereas butene units favor crystallization of the γ and α forms at low and high concentrations, respectively.

The crystallization of the γ form of iPP is, therefore, not only related to the value of the average length of the regular fully isotactic propylene sequences $\langle L_{iPP} \rangle$, but is also related to the different degrees of inclusion of stereodeflects and constitutional defects in the crystals of the α and γ forms of iPP.

Stereodeflects, regiodeflects, and constitutional defects play a double role. The first effect that favors crystallization of the γ form is the interruption of the regular isotactic propylene sequences with shortening of the average length of the regular isotactic sequences $\langle L_{iPP} \rangle$. The second effect is due to the possible inclusion of defects in the crystals of the polymorphic forms of iPP that favors crystallization of the α or γ forms depending on which of the two forms better tolerates the defect within its crystalline lattice.

For iPPet copolymers, ethylene and *rr* stereodeflects are probably more easily included in crystals of the γ form and in α/γ disordered modifications of the γ form, and hence, they favor crystallization of the γ form. In iPPet copolymers and in stereodeflective iPP homopolymers, the effects of crystal inclusion and of shortening of the regular propylene sequences produce the same result of favoring the crystallization of the γ form.

In the case of iPPBu copolymers, butene units are probably included without differentiation in crystals of the α and γ forms, but probably more easily in the α form at high concentrations. Therefore, at low butene concentration, up to nearly 10 mol %, the effect of shortening the length of regular propylene sequences prevails and induces crystallization of the γ form. For higher butene concentrations the effect of inclusion of butene units in crystals of the α form prevails over that of the shortening of $\langle L_{iPP} \rangle$, producing a decrease of the amount of the γ form and, then, a crystallization of the pure α form for butene content higher than 30 mol %.

Acknowledgment. Financial support from Basell Polyolefins, Ferrara (Italy), is gratefully acknowledged. We thank Riccardo Frabetti for producing the polymer samples and Dr. D. Lilge of Basell for the SEC data.

Supporting Information Available: Text showing the experimental details and figure depicting some ^{13}C NMR spectra of

copolymer samples and DSC heating curves. This material is available free of charge via the Internet at <http://pubs.acs.org>.

References and Notes

- (1) Fischer, D.; Mülhaupt, R. *Macromol. Chem. Phys.* **1994**, *195*, 1433.
- (2) Thomann, R.; Wang, C.; Kressler, J.; Mülhaupt, R. *Macromolecules* **1996**, *29*, 8425.
- (3) Alamo, R. G.; Kim, M. H.; Galante, M. J.; Isasi, J. R.; Mandelkern, L. *Macromolecules* **1999**, *32*, 4050.
- (4) VanderHart, D. L.; Alamo, R. G.; Nyden, M. R.; Kim, M. H.; Mandelkern, L. *Macromolecules* **2000**, *33*, 6078.
- (5) Nyden, M. R.; Vanderhart, D. L.; Alamo, R. G. *Comput. Theor. Polym. Sci.* **2001**, *11*, 175.
- (6) Thomann, R.; Semke, H.; Maier, R. D.; Thomann, Y.; Scherble, J.; Mülhaupt, R.; Kressler, J. *Polymer* **2001**, *42*, 4597.
- (7) Auriemma, F.; De Rosa, C.; Boscatto, T.; Corradini, P. *Macromolecules* **2001**, *34*, 4815.
- (8) De Rosa, C.; Auriemma, F.; Circelli, T.; Waymouth, R. M. *Macromolecules* **2002**, *35*, 3622.
- (9) Auriemma, F.; De Rosa, C. *Macromolecules* **2002**, *35*, 9057.
- (10) De Rosa, C.; Auriemma, F.; Circelli, T.; Longo, P.; Boccia, A. C. *Macromolecules* **2003**, *36*, 3465.
- (11) De Rosa, C.; Auriemma, F.; Perretta, C. *Macromolecules* **2004**, *37*, 6843.
- (12) De Rosa, C.; Auriemma, F.; Di Capua, A.; Resconi, L.; Guidotti, S.; Camurati, I.; Nifant'ev, I. E.; Laishevstev, I. P. *J. Am. Chem. Soc.* **2004**, *126*, 17040.
- (13) De Rosa, C.; Auriemma, F.; Spera, C.; Talarico, G.; Tarallo, O. *Macromolecules* **2004**, *37*, 1441.
- (14) De Rosa, C.; Auriemma, F.; Spera, C.; Talarico, G.; Gahleitner, M. *Polymer* **2004**, *45*, 5875.
- (15) De Rosa, C.; Auriemma, F.; Spera, C. *Macromol. Symp.* **2004**, *218*, 113.
- (16) De Rosa, C.; Auriemma, F.; De Lucia, G.; Resconi, L. *Polymer* **2005**, *46*, 9461. De Rosa, C.; Auriemma, F. *J. Am. Chem. Soc.* **2006**, *128*, 11024. De Rosa, C.; Auriemma, F. *Lect. Notes Phys.* **2007**, *714*, 345.
- (17) De Rosa, C.; Auriemma, F.; Paolillo, M.; Resconi, L.; Camurati, I. *Macromolecules* **2005**, *38*, 9143.
- (18) De Rosa, C.; Auriemma, F.; Resconi, L. *Macromolecules* **2005**, *38*, 10080.
- (19) Auriemma, F.; De Rosa, C. *Macromolecules* **2006**, *39*, 7635. Auriemma, F.; De Rosa, C.; Corradi, M. *Adv. Mater.* **2007**, *19*, 871.
- (20) Resconi, L.; Cavallo, L.; Fait, A.; Piemontesi, F. *Chem. Rev.* **2000**, *100*, 1253.
- (21) Turner-Jones, A. *Polymer* **1966**, *7*, 23. Turner-Jones, A. *Polymer* **1971**, *12*, 487.
- (22) (a) Cimmino, S.; Martuscelli, E.; Nicolais, L.; Silvestre, C. *Polymer* **1978**, *19*, 1222. (b) Crispino, L.; Martuscelli, E.; Pracella, M. *Makromol. Chem.* **1980**, *181*, 1747. (c) Cavallo, P.; Martuscelli, E.; Pracella, M. *Polymer* **1997**, *18*, 891.
- (23) Starkweather, H. W., Jr.; Van-Catledge, F. A.; MacDonald, R. N. *Macromolecules* **1982**, *15*, 1600.
- (24) Guidetti, G. P.; Busi, P.; Giulianetti, I.; Zanetti, R. *Eur. Polym. J.* **1983**, *19*, 757.
- (25) Busico, V.; Corradini, P.; De Rosa, C.; Di Benedetto, E. *Eur. Polym. J.* **1985**, *21*, 239.
- (26) Avella, M.; Martuscelli, E.; Della Volpe, G.; Segre, A.; Rossi, E.; Simonazzi, T. *Makromol. Chem.* **1986**, *187*, 1927.
- (27) (a) Marigo, A.; Marega, C.; Zanetti, R.; Paganetto, G.; Canossa, E.; Coletta, F.; Gottardi, F. *Makromol. Chem.* **1989**, *190*, 2805. (b) Marega, C.; Marigo, A.; Saini, R.; Ferrari, P. *Polym. Int.* **2001**, *50*, 442. (c) Marigo, A.; Causin, V.; Marega, C.; Ferrari, P. *Polym. Int.* **2004**, *53*, 2001.
- (28) Monasse, B.; Haudin, J. M. *Colloid Polym. Sci.* **1988**, *266*, 679.
- (29) Zimmermann, H. J. *J. Macromol. Sci. Phys.* **1993**, *B(32)2*, 141.
- (30) Mezghani, K.; Phillips, P. J. *Polymer* **1995**, *35*, 2407. Dimenska, A.; Phillips, P. J. *Polymer* **2006**, *47*, 54445.
- (31) Hingmann, R.; Rieger, J.; Kersting, M. *Macromolecules* **1995**, *28*, 3801.
- (32) Morini, G.; Albizzati, E.; Balbontin, G.; Mingozzi, I.; Sacchi, M. C.; Forlini, F.; et al. *Macromolecules* **1996**, *29*, 5770.
- (33) Laihonon, S.; Gedde, U. W.; Werner, P. E.; Martinez-Salazar, J. *Polymer* **1997**, *38*, 361. Laihonon, S.; Gedde, U. W.; Werner, P. E.; Westdahl, M.; Jääskeläinen, P.; Martinez-Salazar, J. *Polymer* **1997**, *38*, 371.
- (34) Pérez, E.; Benavente, R.; Bello, A.; Peña, J. M.; Zucchi, D.; Sacchi, M. C. *Polymer* **1997**, *38*, 5411.
- (35) Abiru, T.; Mizuno, A.; Weigand, F. *J. Appl. Polym. Sci.* **1998**, *68*, 1493.

- (36) Feng, Y.; Jin, X.; Hay, J. N. *J. Appl. Polym. Sci.* **1998**, *68*, 381. Feng, Y.; Hay, J. N. *Polymer* **1998**, *39*, 6589. Xu, J.; Feng, Y. *Eur. Polym. J.* **2000**, *36*, 867.
- (37) Zhao, Y.; Vaughan, A. S.; Sutton, S. J.; Swingler, S. G. *Polymer* **2001**, *42*, 6599.
- (38) Foresta, T.; Piccarolo, S.; Goldbeck-Wood, G. *Polymer* **2001**, *42*, 1167.
- (39) Yang, S. L.; Xu, Z. K.; Feng, L. X. *Makromol. Chem. Macromol. Symp.* **1992**, *63*, 233. Xu, Z. K.; Feng, L. X.; Wang, D.; Yang, S. L. *Makromol. Chem.* **1992**, *192*, 1835.
- (40) Sugano, T.; Gotoh, Y.; Fujita, T. *Makromol. Chem.* **1992**, *193*, 43.
- (41) Arnold, M.; Henschke, O.; Knorr, J. *Macromol. Chem. Phys.* **1996**, *197*, 563.
- (42) Arnold, M.; Bornemann, S.; Köller, F.; Menke, T. J.; Kressler, J. *Macromol. Chem. Phys.* **1998**, *199*, 2647.
- (43) Busse, K.; Kressler, J.; Maier, R. D.; Scherble, J. *Macromolecules* **2000**, *33*, 8775.
- (44) (a) Forlini, F.; Fan, Z.-Q.; Tritto, I.; Locatelli, P.; Sacchi, M. C. *Macromol. Chem. Phys.* **1997**, *198*, 2397. (b) Tritto, I.; Donetti, R.; Sacchi, M. C.; Locatelli, P.; Zanoni, G. *Macromolecules* **1999**, *32*, 264. (c) Pérez, E.; Zucchi, D.; Sacchi, M. C.; Forlini, F.; Bello, A. *Polymer* **1999**, *40*, 675. (d) Forlini, F.; Tritto, I.; Locatelli, P.; Sacchi, M. C.; Piemontesi, F. *Macromol. Chem. Phys.* **2000**, *201*, 401. (e) Sacchi, M. C.; Forlini, F.; Losio, S.; Tritto, I.; Wahner, U. M.; Tincul, I.; Joubert, D. J.; Sadiku, E. R. *Macromol. Chem. Phys.* **2003**, *204*, 1643. (f) Wahner, U. M.; Tincul, I.; Joubert, D. J.; Sadiku, E. R.; Forlini, F.; Losio, S.; Tritto, I.; Sacchi, M. C. *Macromol. Chem. Phys.* **2003**, *204*, 1738. (g) Costa, G.; Stagnaro, P.; Trefiletti, V.; Sacchi, M. C.; Forlini, F.; Alfonso, G. C.; Tincul, I.; Wahner, U. M. *Macromol. Chem. Phys.* **2004**, *205*, 383. (h) Sacchi, M. C.; Forlini, F.; Tritto, I.; Stagnaro, P. *Macromol. Chem. Phys.* **2004**, *205*, 1804. (i) Sacchi, M. C.; Forlini, F.; Losio, S.; Tritto, I.; Costa, G.; Stagnaro, P.; Tincul, I.; Wahner, U. M. *Macromol. Symp.* **2004**, *213*, 57. (l) Stagnaro, P.; Costa, G.; Trefiletti, V.; Canetti, M.; Forlini, F.; Alfonso, G. C. *Macromol. Chem. Phys.* **2006**, *207*, 2128.
- (45) Kim, I. *Macromol. Rapid Commun.* **1998**, *19*, 299. Kim, I.; Kim, Y. I. *Polym. Bull. (Berlin)* **1998**, *40*, 415.
- (46) Alamo, R. G.; Isasi, J. R.; Kim, M.-H.; Mandelkern, L.; VanderHart, D. L. *Polym. Mater. Sci. Eng. Proc.* **1999**, *81*, 346.
- (47) Alamo, R. G.; VanderHart, D. L.; Nyden, M. R.; Mandelkern, L. *Macromolecules* **2000**, *33*, 6094.
- (48) Hosier, I. L.; Alamo, R. G.; Estes, P.; Isasi, G. R.; Mandelkern, L. *Macromolecules* **2003**, *36*, 5623.
- (49) Hosier, I. L.; Alamo, R. G.; Lin, J. S. *Polymer* **2004**, *45*, 3441.
- (50) Alamo, R. G.; Ghosal, A.; Chatterjee, J.; Thompson, K. L. *Polymer* **2005**, *46*, 8774.
- (51) Fan, Z.; Yasin, T.; Feng, L. *J. Polym. Sci., Part A* **2000**, *38*, 4299.
- (52) Van, Reenen, A. J.; Brull, R.; Wahner, U. M.; Pasch, H. *Polym. Prepr.* **2000**, *41*, 496. Brull, R.; Pasch, H.; Rauberheimer, H. G.; Sanderson, R. D.; Wahner, U. M. *J. Polym. Sci., Part A: Polym. Chem.* **2000**, *38*, 2333. Van Reenen, A. J.; Brull, R.; Wahner, U. M.; Rauberheimer, H. G.; Sanderson, R. D.; Pasch, H. *J. Polym. Sci., Part A: Polym. Chem.* **2000**, *38*, 4110.
- (53) Lovisi, H.; Tavares, M. I. B.; da Silva, N. M.; de Menezes, S. M. C.; de Santa, Maria, L. C.; Coutinho, F. M. B. *Polymer* **2001**, *42*, 9791.
- (54) Shin, Y.-W.; Uozumi, T.; Terano, M.; Nitta, K.-H. *Polymer* **2001**, *42*, 9611.
- (55) Shin, Y.-W.; Hashiguchi, H.; Terano, M.; Nitta, K.-H. *J. Appl. Polym. Sci.* **2004**, *92*, 2949.
- (56) Hosoda, S.; Hori, H.; Yada, K.; Tsuji, M.; Nakahara, S. *Polymer* **2002**, *43*, 7451.
- (57) Fujiyama, M.; Inata, H. *J. Appl. Polym. Sci.* **2002**, *85*, 1851.
- (58) Xu, J.-T.; Xue, L.; Fan, Z.-Q. *J. Appl. Polym. Sci.* **2004**, *93*, 1724.
- (59) Poon, B.; Rogunova, M.; Chum, S. P.; Hiltner, A.; Baer, E. *J. Polym. Sci., Polym. Phys.* **2004**, *42*, 4357.
- (60) Poon, B.; Rogunova, M.; Hiltner, A.; Baer, E.; Chum, S. P.; Galeski, A.; Piorkowska, E. *Macromolecules* **2005**, *38*, 1232.
- (61) Palza, H.; López-Majada, J. M.; Quijada, R.; Benavente, R.; Pérez, E.; Cerrada, M. L. *Macromol. Chem. Phys.* **2005**, *206*, 1221.
- (62) López-Majada, J. M.; Palza, H.; Guevara, J. L.; Quijada, R.; Martínez, M. C.; Benavente, R.; Pereña, J. M.; Pérez, E.; Cerrada, M. L. *J. Polym. Sci., Polym. Phys. Ed.* **2006**, *44*, 1253.
- (63) De Rosa, C.; Auriemma, F.; Corradini, P.; Tarallo, O.; Dello Iacono, S.; Ciaccia, E.; Resconi, L. *J. Am. Chem. Soc.* **2006**, *128*, 80.
- (64) De Rosa, C.; Dello Iacono, S.; Auriemma, F.; Ciaccia, E.; Resconi, L. *Macromolecules* **2006**, *39*, 6098.
- (65) (a) De Rosa, C.; Esposito, G.; Auriemma, F.; Resconi, L. *Proceeding of the XVII Italian Meeting of Science and Technology of Macromolecules* 2005; p 225. (b) De Rosa, C.; Piscitelli, F.; Schiavo, L.; Auriemma, F.; Resconi, L. *Proceeding of the XVII Italian Meeting of Science and Technology of Macromolecules*; 2005; p 226.
- (66) Lotz, B.; Ruan, J.; Thierry, A.; Alfonso, G. C.; Hiltner, A.; Baer, E.; Piorkowska, E.; Galeski, A. *Macromolecules* **2006**, *39*, 5777.
- (67) Toki, S.; Sics, I.; Burger, C.; Fang, D.; Liu, L.; Hsiao, B. S.; Datta, S.; Tsou, A. H. *Macromolecules* **2006**, *39*, 3588.
- (68) Bingel, C.; Goeres, M.; Fraaije, V.; Winter, A. (Targor) *Int. Pat. Appl. WO* 1998/040331.
- (69) Resconi, L.; Ciaccia, E.; Fait, A. (Basell: Italy) *Int. Pat. Appl. WO* 2004/092230.
- (70) Stehling, U.; Diebold, J.; Kirsten, R.; Roell, W.; Brintzinger, H.-H.; Juengling, S.; Mülhaupt, R.; Langhauser, F. *Organometallics* **1994**, *13*, 964. Langhauser, F.; Kerth, J.; Kersting, M.; Koelle, P.; Lilge, D.; Mueller, P. *Angew. Makromol. Chem.* **1994**, *223*, 155.
- (71) Resconi, L.; Guidotti, S.; Camurati, I.; Frabetti, R.; Focante, F.; Nifant'ev, I. E.; Laishevstev, I. P. *Macromol. Chem. Phys.* **2005**, *206*, 1405 and references therein.
- (72) Covezzi, M.; Fait, A. (Basell: Italy) *PCT Int. Appl. WO* 01/44319, 2001.
- (73) Randall, J. C. *Macromol. Chem. Phys.* **1989**, *C29*, 201.
- (74) Tritto, I.; Fan, Z.; Locatelli, P.; Sacchi, M.; Camurati, I.; Galimberti, M. *Macromolecules* **1995**, *28*, 3342.
- (75) Kakugo, M.; Naito, Y.; Mizunuma, K.; Miyatake, T. *Macromolecules* **1982**, *15*, 1150.
- (76) Carman, C. J.; Harrington, R. A.; Wilkes, C. E. *Macromolecules* **1977**, *10*, 536.
- (77) Randall, J. C. *Macromolecules* **1978**, *11*, 592.
- (78) Brückner, S.; Meille, S. V. *Nature (London)* **1989**, *340*, 455. Meille, S. V.; Brückner, S.; Porzio, W. *Macromolecules* **1990**, *23*, 4114.
- (79) Natta, G.; Corradini, P. *Nuovo Cimento Suppl.* **1960**, *15*, 40.
- (80) *Cerius² Modeling Environment*; Molecular Simulations Inc.: San Diego, CA 1999.
- (81) (a) Dinur, U.; Hagler, A. T. New Approaches to Empirical Force Fields. In *Review of Computational Chemistry*, 1991; Chapter 4. (b) Maple, J. R.; Dinur, U.; Hagler, A. T. *Proc. Natl. Acad. Sci. U.S.A.* **1988**, *85*, 5350. (c) Sun, H.; Mumby, S. J.; Maple, J. R.; Hagler, A. T. *J. Am. Chem. Soc.* **1994**, *116*, 2978. (d) Sun, H. *Macromolecules* **1994**, *26*, 5924. (e) Sun, H. *Macromolecules* **1995**, *28*, 701.
- (82) Hikosaka, M.; Seto, T. *Polym. J.* **1973**, *5*, 111.
- (83) Khoury, F. *J. Res. Natl. Bur. Stand* **1966**, *70A*, 29. Khoury, F.; Passaglia, E. In *Treatise on Solid State Chemistry*; Hannay, N. B., Ed.; Plenum: New York, 1976, Vol. 3, p 335 [Chapter 6].
- (84) Lotz, B.; Wittmann, J. C. *J. Polym. Sci., Polym. Phys. Ed.* **1986**, *24*, 1541.
- (85) Lotz, B.; Graff, S.; Straupé, C.; Wittmann, J. C. *Polymer* **1991**, *32*, 2902.
- (86) Brandrup, J.; Immergut, E. H.; Grulke, E. A. *Polymer Handbook*; John Wiley: New York, 1999.

MA070409+